2018

DEVELOPMENT OF AN INTEGRATED HYDRODYNAMIC AND COASTAL RISK ASSESSMENT MODEL FOR CHARLESTOWN, RI

Christopher J. Small
University of Rhode Island, chris.small.401@gmail.com

DEVELOPMENT OF AN INTEGRATED HYDRODYNAMIC AND COASTAL RISK ASSESSMENT MODEL FOR CHARLESTOWN, RI

BY

CHRISTOPHER J. SMALL

A THESIS SUBMITTED IN PARTIAL FULFILLMENT OF THE

REQUIREMENTS FOR THE DEGREE OF

MASTER OF SCIENCE

IN

OCEAN ENGINEERING

UNIVERSITY OF RHODE ISLAND

2018

MASTER OF SCIENCE THESIS

OF

CHRISTOPHER J. SMALL

APPROVED:

Thesis Committee:

Major Professor M. Reza Hashemi

Annette Grilli

Emi Uchida

Malcolm Spaulding

Nasser H. Zawia

DEAN OF THE GRADUATE SCHOOL

UNIVERSITY OF RHODE ISLAND

2018

ABSTRACT

The Northeast Coast of the United States faces the possible damaging effects of storm surge, waves, and wind due to Atlantic tropical and extratropical storms each year. Historically, there have been several significant storm events that produced substantial levels of damage to the region, most notably the Great Atlantic Hurricane of 1938, Hurricane Carol, Hurricane Bob, and most recently Hurricane Sandy (2012). The objective of this study was to develop an integrated modeling system that could be used as a forecasting tool to evaluate and communicate the risk coastal communities face from these aforementioned hazards. This system utilizes the ADvanced CIRCulation (ADCIRC) model for storm surge predictions and the Simulating WAves Nearshore (SWAN) model for the wave environment. The two models are tightly coupled, passing information to each other and computing over the same unstructured domain, allowing for the most accurate representation of the physical storm processes. The coupled SWAN+ADCIRC model was extensively validated for Rhode Island coastal waters, and has been set up to perform real-time forecast simulations. Modeled storm parameters are then passed to a coastal risk assessment tool. This tool is universally applicable, and generates spatial structural damage estimate maps on an individual structure basis for a specific study area. The required inputs are detailed information about the individual structures, inundation levels, and wave heights for the selected region. Additionally, an option for estimating wind damage to structures was incorporated.

Once developed, the integrated coastal risk assessment system was tested and applied to Charlestown, a small vulnerable coastal town along the southern shore of Rhode Island. The developed system was tested for Hurricane Sandy and a synthetic 100-year storm. In both storm cases, a dune intact and dune eroded scenario were simulated. For the dune intact scenario the current dune profile present was used, while for the dune eroded case a 100-year storm dune eroded profile was used. The resulting damage maps

for Charlestown clearly show that the dune eroded scenarios affected more structures, and increased the severity of the estimated damage. The system was also tested in forecast mode for two large Nor'Easters, Stella (March 2017) and Riley (March 2018). The results showed the coupled model performed well in forecast mode when compared to observations. Neither Nor'Easter produced damage to the study area, which was why the 100-year storm was used as a hypothetical future storm. This coastal risk assessment system is unique because of its ability to provide real-time forecasting of structural damage to a region. Ideally, this system's estimated damage maps will be used by coastal zone and emergency managers to identify high risk areas in coastal communities, allowing for the determination of the best adaptation and mitigation strategies.

ACKNOWLEDGMENTS

I would first like to thank my advising professor, Dr. Reza Hashemi, for providing me with the opportunity to continue my education by taking me on as a master's student. Your guidance was vital to this research process, and you have helped me to improve both my academic and professional abilities. I would also like to extend my gratitude to Dr. Malcolm Spaulding and Dr. Christopher Baxter, who have helped advise me since my undergraduate senior capstone project, and even assisted getting me into graduate program on very late notice.

I also want to acknowledge the members and chair of my committee, Dr. Annette Grilli, Dr. Emi Uchida, Dr. Malcolm Spaulding, and Dr. Aaron Bradshaw. Thank you for your time, the experience, and most importantly your eventual advice and feedback on my thesis.

Lastly, I would like to thank my family, close friends, and fellow students. Without your support this process would have been much more difficult, and significantly less enjoyable. I am forever grateful for you guys.

- Christopher J. Small

TABLE OF CONTENTS

Page

LIST OF FIGURES

Figure **Page**

Figure **Page**

LIST OF TABLES

MANUSCRIPT 1

Development of an Integrated Hydrodynamic and Coastal Risk Assessment Model for Charlestown, RI

1.1 Introduction

1.1.1 Risk Overview and Background

The Northeast Coast of the United States is located in a precarious position when observing the typical storm tracks for Atlantic tropical storms. The majority of Atlantic tropical storms develop in the Atlantic near Cape Verde, move westward, and then begin to bend northward traveling along the East Coast of the United States. As they move northward along the coast, they begin to present a greater risk to the entire Northeast, and therefore Rhode Island. Fortunately, in most cases the storms typically turn eastward back out to the ocean before they become a significant problem for this area. Although this is the norm for most storms, it is not always the case. There have been historical storms that made landfall or traveled closely along the coastline producing significant levels of damage in Rhode Island. The most recent was Hurricane Sandy, which did not make landfall in Rhode Island, but had such a large radius of maximum wind that it still produced a strong storm surge in Rhode Island, resulting in damage to coastal communities. Additional historical storms that produced considerable damage to Rhode Island were the Great New England Hurricane (1938), Hurricane Carol (1954), and Hurricane Bob (1991). The tracks of these historical storms can be seen in Figure 1.1. Hurricane Bob passed directly through Narragansett Bay, but the Great New England Hurricane of 1938 was still the worst storm to impact Rhode Island. This storm made landfall to the west of Rhode Island, placing the state in the front right quadrant of the storm where the storm effects are the strongest due to the counter-clockwise rotation of the winds. The destruction from this specific storm was amplified due to an increased high tide occurring as a result of the autumnal equinox and a full moon.

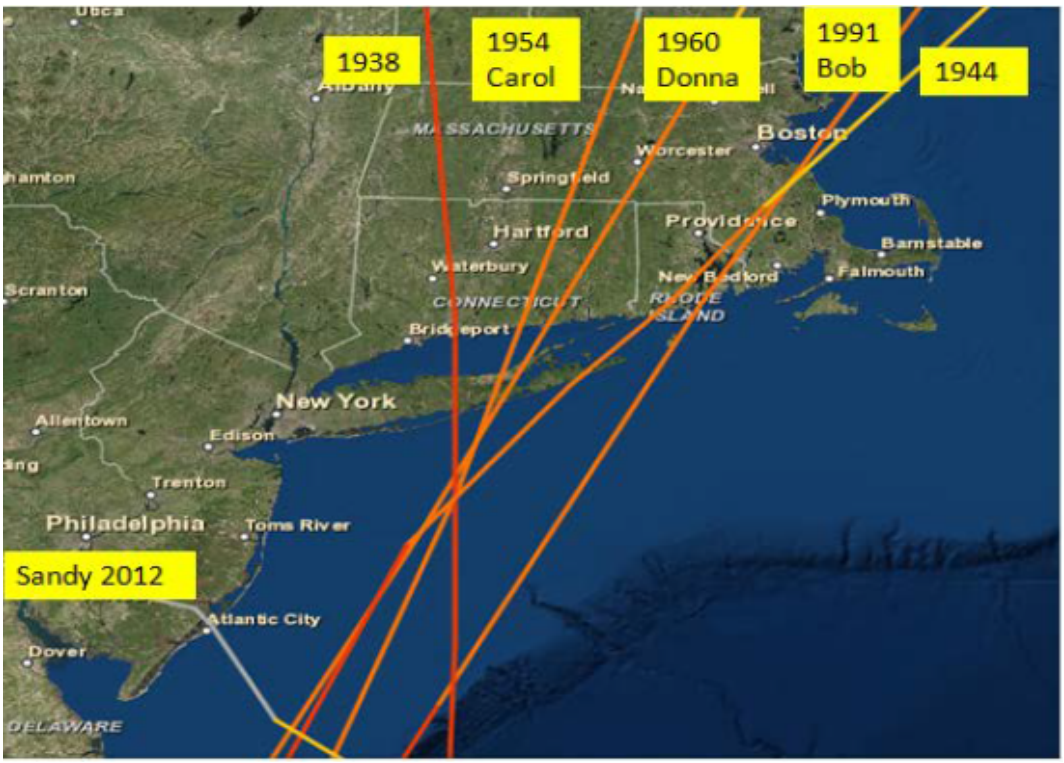

Fig. 1.1. Storm tracks of historical hurricanes that impacted Rhode Island (NHC, 2018).

Rhode Island is becoming more vulnerable to these hazards as time passes. Climate change is expected to begin increasing the intensity and frequency of these events, which may lead to larger impacts from these storms on coastal communities (Parris et al., 2012). One such change is sea-level rise (SLR), which the National Oceanic and Atmospheric Administration (NOAA) has predicted SLR of around 3.4 m, according to their extreme rate, by the year 2100 for the state, as displayed in Figure 1.2 (NOAA, 2018). The culmination of these effects means that storms which would originally cause little to no damage will now begin to present a larger risk. This amplifying risk puts a higher number of structures, infrastructure, and most importantly residents in danger.

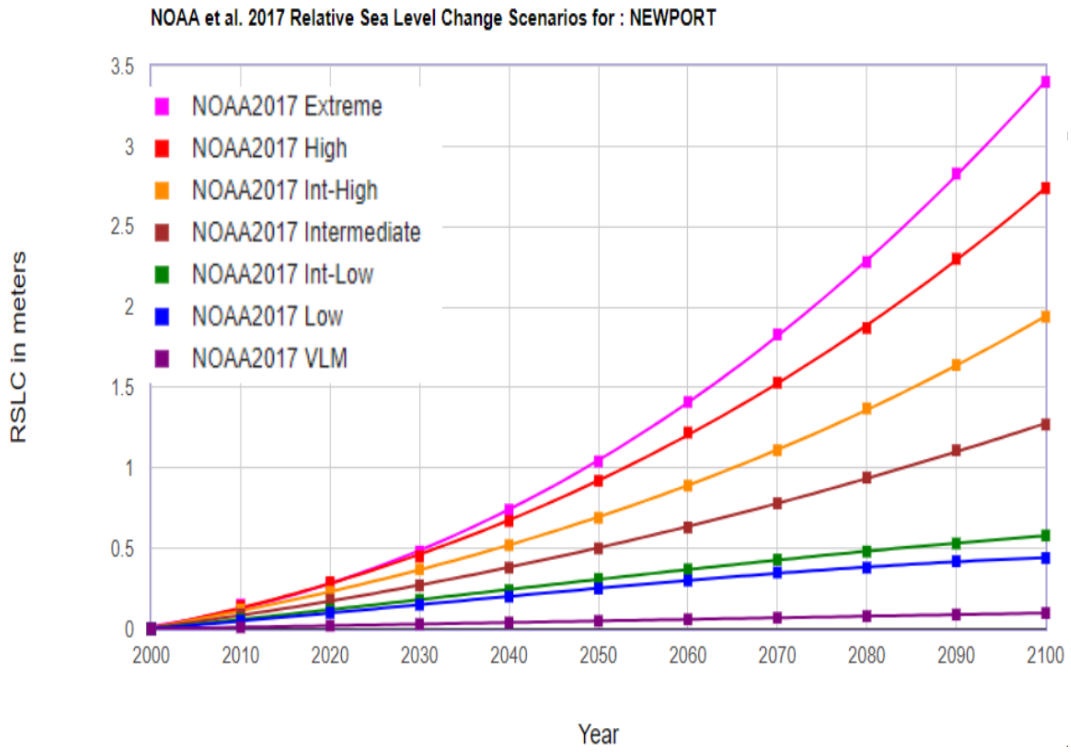

Fig. 1.2. NOAA's relative sea-level change (RSCL) predictions for SLR at Newport, RI. RSCL is SLR specific to a location/region (NOAA, 2018).

For these reasons, it is necessary to have a method to accurately forecast the storm surge and wave effects of a given storm to convey the risk to emergency management planners, government officials, and the public. This has lead to studies involving the development of hurricane forecast systems along the east coast that utilize a suite of different models and approaches. The National Weather Service (NWS) branch of NOAA currently implements the storm surge model Sea, Lake, and Overland Surges from Hurricanes (SLOSH) in real-time when a hurricane is threatening. The SLOSH model contains 38 basins that correspond to 38 specific coastal areas along of the U.S. coasts (Glahn et al., 2009). This forecast system is forced using the National Hurricane Center's (NHC) meteorological forecasts. SLOSH does have a basin that includes Rhode Island, but the resolution is very coarse. SLOSH is also considered a simplistic storm surge model as the tidal input is decoupled and not time dependent. Another forecast

system in place is the North Carolina Forecast System (NCFS), which implements the ADvanced CIRCulation (ADCIRC) model (Mattocks and Forbes, 2008). The domain for this system has high resolution around North Carolina, and encompasses the Western Atlantic, the Gulf of Mexico, and the Caribbean Sea. The wind forcing for this model utilizes a synthetic asymmetric Holland gradient wind model to construct a tropical storm vortex from the NHC forecasts (Mattocks and Forbes, 2008). While this system performs well and includes Rhode Island the resolution around the state is not sufficient, which is expected as the focus is North Carolina.

The last two forecast systems did not include waves, and therefore were missing a significant portion of the risk that tropical storms present. Another tool that has been created is the ADCIRC Surge Guidance System (ASGS), which implements the wave model Simulation WAves Nearshore (SWAN) coupled with the circulation model ADCIRC. This system can be forced using two different wind products. The first is from the National Centers for Environmental Prediction (NCEP), which has a North American Mesoscale (NAM) model providing a 3.5 day forecast at a resolution of 12km. The second is similar to the North Carolina study, and utilizes a Generalized Asymmetric Holland Model (GAHM) with the NHC forecast data (Fleming et al., 2008). This system is meant to be portable, and in theory could be applied to a domain with high resolution in Rhode Island. However, the current domain implemented in this system has poor resolution in Rhode Island. Finally, the last forecast system reviewed was the Northeast Coastal Ocean Forecast System (NECOFS), which is an integrated atmospheric-ocean forecast model system developed for the northeast covering the area from central New Jersey to Nova Scotia. This system includes wind forcing from the mesoscale meteorological model Weather Research and Forecasting (WRF), the wave model SWAVE (finite-volume modification of SWAN), and a Finite-Volume Community Ocean Model (FVCOM) for ocean circulation (Beardsley and Chen, 2014). There are

several domains to this system due to the number of models, with the finest having extremely high resolution in the Massachusetts area (up to 10m). The section of the domain that covers Rhode Island has decent resolution, and was used as the starting point for the forecast system utilized in this study. The forecast system for this study implements the FVCOM Gulf of Maine version 4 (GOM4) mesh developed by the University of Massachusetts Dartmouth (Chen et al., 2006). This mesh's resolution was increased to be much finer around Rhode Island. The details of this forecast system developed for Rhode Island will be discussed later in the paper.

Not only is it important to have a system in place that is capable of accurately forecasting storm surge, waves, and wind, but it is also important to have a methodology for transferring these hazards into terms of risk for coastal communities. In most cases, studies will utilize fragility curves or depth damage functions. The wind loading and fragility curves are the most well developed (Ellingwood et al., 2004; Lee and Rosowsky, 2005; Li and Ellingwood, 2006; Hamid et al., 2010; Li et al., 2011; Pinelli et al., 2011). These curves are the result of years of laboratory and field measurements, engineering designs and analyses, and numerical simulations (Tomiczek et al., 2013). As a result, the wind damage can be estimated with reasonable accuracy. The attempts to quantify storm surge damage are newer, more empirical based, and contain more uncertainty. These attempts usually involve functions quantifying the relationship between surge depth and damage (Jonkman et al., 2008; FEMA, 2012; Tomiczek et al., 2013; USACE, 2015). In these studies, the functions were developed based on historical damage to structures as a result of storm surge. Due to the infrequency of historical storms resulting in damage these damage functions are not as well developed, and therefore the damage estimates contain substantial uncertainty. The attempts to develop wave damage functions are the newest, and least studied (Tomiczek et al., 2013; USACE, 2015). The largest study to investigate

this damage was the North Atlantic Coast Comprehensive Study (NACCS), performed by the U.S. Army Corps of Engineers (USACE), and involved the generation of wave damage functions based on observed damage from Hurricane Sandy. These functions related wave crest height to structural and content damage. Similar to the storm surge damage functions, these wave damage functions also contain substantial uncertainty. The best possible method for improving the storm surge and wave damage functions would be the implementation of full-scale laboratory testing to closely study the physical relationship between storm surge, waves, and structural damage.

The fragility curves and damage functions are implemented in varying methods for coastal risk assessment. In most cases, the studies do not focus on all the storm effects (i.e. storm surge, waves, wind), and lack a real-time risk forecasting ability. For example, many studies have been published involving the estimation of only wind damage, and are mainly insurance related (Hamid et al., 2010; Li and Ellingwood, 2006). The state of Florida developed an open-source probabilistic assessment of risk in terms of losses to insured buildings due to hurricane winds on a county to state wide scales (Hamid et al., 2010). Another study performed a similar probabilistic assessment of wind damage from hurricanes to residential structures utilizing fragility curves (Li and Ellingwood, 2006). In both cases, the risk assessment may be viable for structures set back from the coast that are only experiencing wind effects, but for coastal structures their results would not be accurate since the damage is not just a function of wind.

In other studies the effects from storm surge and/or waves have been considered. A study in the Netherlands developed a model for the estimation of physical damage caused by floods utilizing depth damage functions (Jonkman et al., 2008). The results from this study were spatial distributions of damage intensity across a coastal community or the entire country, but only from the effects of inundation. Another study was carried

out following Hurricane Ike for the Bolivar Peninsula in Texas to investigate the ability to model damage from storm surge and waves when compared to the actual damage that occurred. The study focused on how different structural characteristics affected the damage, determining the elevation of the structure was the most important factor, and also concluded wave damage dominates (Tomiczek et al., 2013). These studies excluded any effects from wind, and did not involve forecasting. It is noted that this literature review is not exhaustive and the cited papers were simply selected as examples.

For these reasons, there have been efforts to include all the aforementioned hazards from storms into one risk model. The most well-known of which is produced by the Federal Emergency Management Agency (FEMA) called Hazus. This model contains a standardized methodology that allows it to be nationally applicable estimating potential losses from earthquakes, tsunamis, floods, and hurricanes. As a result the flood model can be run for coastal flooding effects and the hurricane model can be run for wind effects (Scawthorn et al., 2006; Vickery et al., 2006). The results of these models identify the high-risk locations and the limits of the expected losses. For coastal risk assessment purposes this system may be adequate, but it relies on readily available data for flooding and wind. This data is not always available and can require external user generation. Hazus also is not developed to be implemented in forecasting purposes.

In the state of Rhode Island, there is currently a developed Coastal Environmental Risk Index (CERI) tool, which implements an inundation model, wave model, and the USACE damage functions to estimate structural damage on an individual structure basis for coastal communities (Small et al., 2016; Spaulding et al., 2016). The outputs from CERI are maps that spatially display the estimated damage for each structure inside the selected study area. The risk assessment for this study was based on the methodology for CERI, with adaptations made to include a damage forecasting option and wind damage option. Damage forecasting was determined to be extremely important because the

previous risk assessment research focused on past events. Emergency planners and government officials require a tool that is capable of providing information about the potential damage of an approaching storm. This risk forecasting tool was developed and originally implemented to Charlestown, RI, but is designed in a way that it is capable of being applied to any coastal community.

1.1.2 Study Area

Charlestown is a coastal town located in southern Rhode Island, shown in Figure 1.3, that is vulnerable to the effects of tropical storms, namely storm surge, waves, wind, and erosion. The town is composed of predominantly low density single family residences, and is located on a barrier system, which leaves its structures and infrastructure at risk to the aforementioned hazards (Spaulding et al., 2016). The town historically has been damaged from storms, and most recently by Hurricane Sandy. Hurricane Sandy occurred in late October of 2012, and produced strong storm surge, large wave heights, and powerful winds. The result of the combination of these storm effects can be viewed in Figure 1.4. This figure shows four images that were taken post Sandy. The images in (a) and (b) were taken very close to Charlestown. Image (a) shows an inlet that formed during Hurricane Sandy allowing for more storm surge and larger wave heights to propagate into the coastal pond, and (b) shows that the dunes were completely eroded and moved backwards into the marsh. The two bottom images in the figure, (c) and (d), show damaged structures that are located in Charlestown.

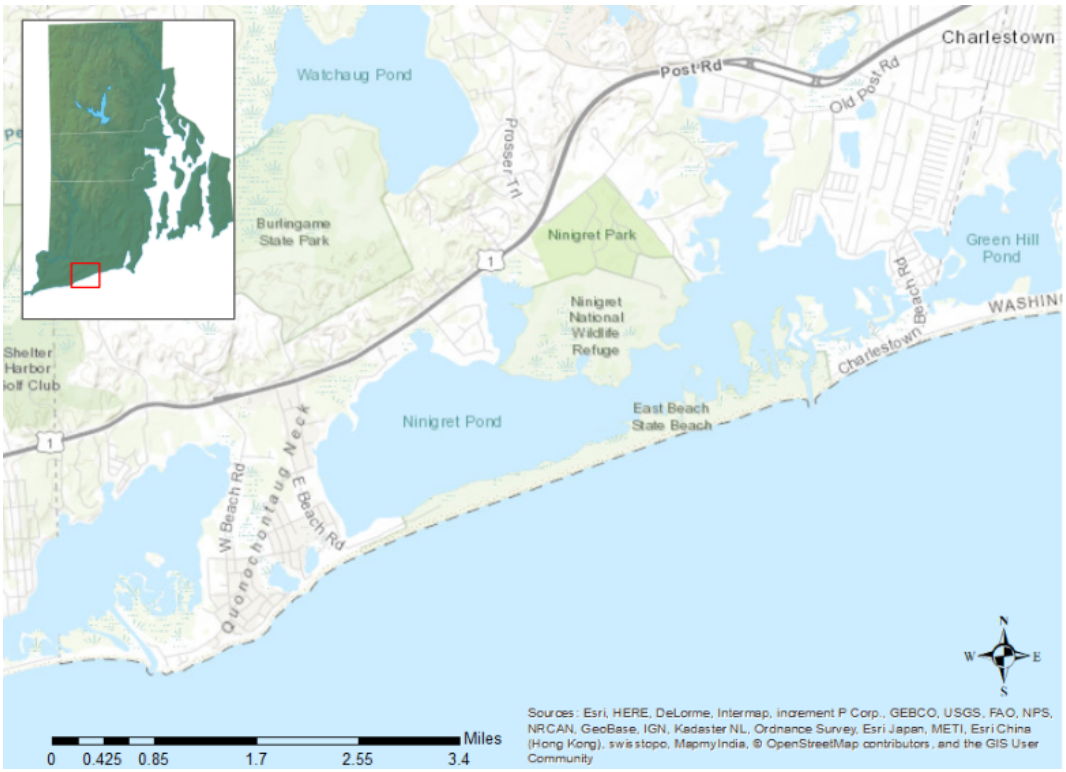

Fig. 1.3. Satellite image of the selected study area of Charlestown, RI. The map insert in the top left of the image shows the study area location in reference to the state, marked in red.

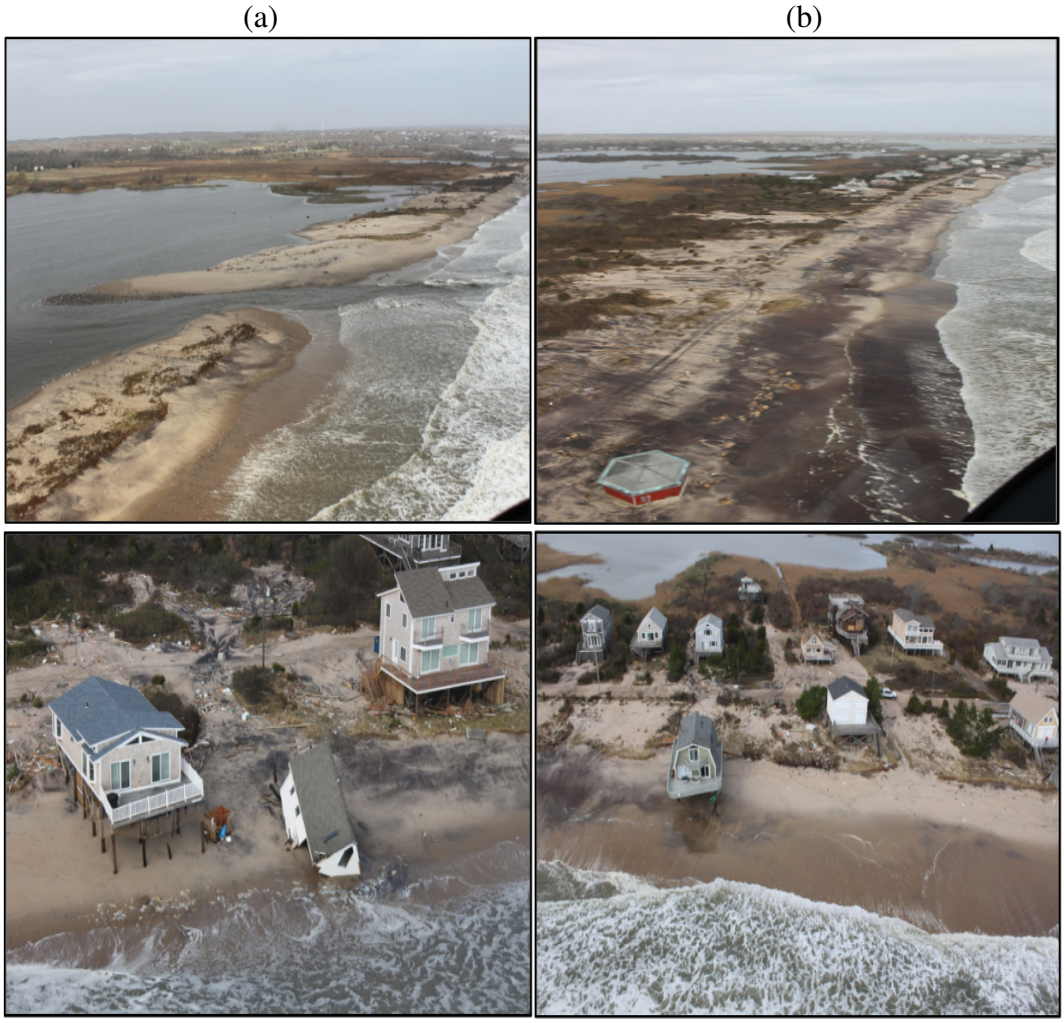

Fig. 1.4. Images taken post Hurricane Sandy near/in Charlestown, RI: (a) inlet that formed to the northeast of the study area; (b) dune system eroded and pushed backwards, also to the northeast; (c) structural damage to a house in the study area; (d) foundation of structure compromised, also in the study area. Photos courtesy of the Rhode Island Department of Transportation.

For these outlined reasons Charlestown was selected as the area of interest for this study. The selected study area is shown in Figure 1.3, both locally and in relation to Rhode Island. As the figure shows the study area is a barrier system with a prominent headland, both of which have a high density of structures located on them. There is also a coastal pond, Ninegret Pond, located behind the barrier system, which can allow for back flooding damage to the structures located further away from the coastline.

1.1.3 Objectives

The overreaching goal of this study was to develop an integrated modeling system to forecast real-time coastal risk assessment on an individual structure basis. This was achieved by completing the three main objectives, which were as follows:

1. Development of an integrated model system to predict storm surge, waves, and damage to a selected coastal region from tropical or extratropical storm events.

2. Apply the model system to a case study of Charlestown, RI, and predict damage for selected historical tropical storms.

3. Demonstrate the capability of the model system to forecast damage.

1.2 Methodology

Key terms have already been used, and will be used throughout this entire study and must be defined. These definitions correspond to how the terminology is used in this study, and may vary in other research. Hazard is defined as a dangerous physical event that may cause loss of life and/or property damage, meaning the storm event and its effects (i.e. storm surge, wave heights, and wind). Vulnerability is defined as susceptibility to loss of life or structural damage from hazards, sometimes referred to as exposure. The final term is risk, which is defined as the combination of hazard and vulnerability. In this paper the risk is identified based on structural damage as a function of a structures vulnerability to the hazard. It is also noted that all water levels and wave heights presented throughout this paper are referenced to mean sea level (MSL). MSL is 0.09 m lower than NAVD88, which is the more commonly used vertical datum.

The integrated modeling system that was developed to perform the risk assessment for this study is composed of several modules, shown in Figure 1.5. Each block of the modeling system shown in the flowchart will be explained in detail throughout this section. The very first step of this system involves making a decision on whether to

perform the risk assessment on a hindcast event (historical storms) or forecast event (future storms).

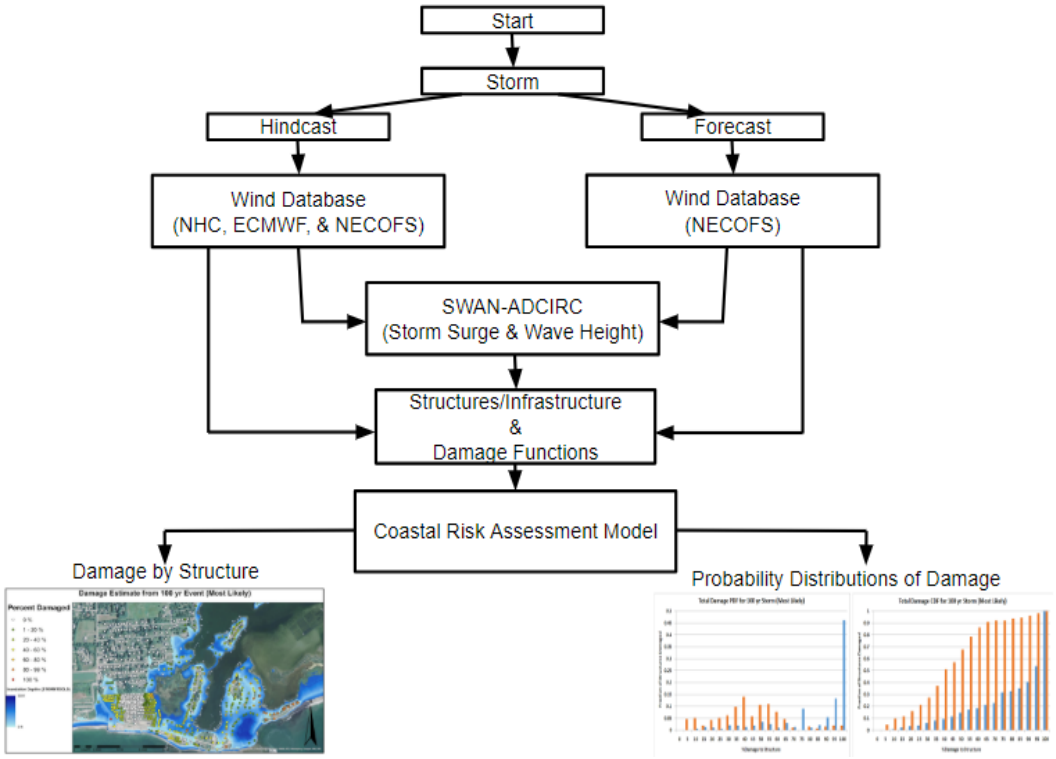

Fig. 1.5. Flowchart of the integrated modeling system for the risk assessment of coastal storms.

1.2.1 Wind Data

The key input for numerical models is the meteorological forcing, which is the primary controlling factor in the prediction of storm surge and wave heights in the model output. This means utilizing the most accurate and realistic wind information is vital to achieving model results that align well with observational data. The wind models that were readily available for this study were from the National Hurricane Center (NHC), which has two products the HURicane DATabase (HURDAT) and Extended Best Track (EBT), the European Center for Medium-Range Weather Forecasting (ECMWF), and the NorthEast Coastal Ocean Forecast System (NECOFS) Weather Research and Forecasting (WRF) winds. In a previous study Torres et al., (2017) investigated the availability and

accuracy of each of the mentioned wind products for Rhode Island, and it was determined that the best wind product for the present study area was the NECOFS WRF model (Torres et al., 2017).

The NECOFS WRF wind product is forced by a global North Atlantic Mesoscale (NAM) weather model. The actual WRF model contains three grid domains with varying resolution, the basin domain with 27 km resolution, the regional domain with 9 km resolution, and the local domain with 3 km resolution. For this model the regional and local domains are run simultaneously through two-way interaction, which is a nesting method in which the input from the coarse domain (regional) is included via boundaries on the smaller nested domain (local). The nested domain results are then feedback to the coarse domain (Chen et al., 2006). Three days of hindcast wind data and three days of forecast wind data are provided by this model, which is updated automatically daily. This intricate model setup is one of the reasons that this wind data is suitable for Rhode Island, another reason is the high resolution (3 km) of the local domain, which covers the case study area. This wind forcing was used throughout this study, both in hindcast and forecast risk assessment modes.

1.2.2 Numerical Models

Regional Wave Model

The wave model implemented for this study was SWAN, which is a third-generation discrete spectral wave model that characterizes the evolution of the two-dimensional wave action density spectrum. In this model the action density spectrum ($N = E/\sigma$) is used because action density is conserved in the presence of ambient currents, whereas the the energy density ($E(\sigma, \theta)$) is not (Booij et al., 1999). SWAN solves for the evolution of the wave spectrum by solving the spectral action balance equation, shown in Equation 1.1 (Booij et al., 1999; Ris et al., 1999).

$$\frac{\partial}{\partial t}N + \frac{\partial}{\partial x}c_x N + \frac{\partial}{\partial y}c_y N + \frac{\partial}{\partial \sigma}c_\sigma N + \frac{\partial}{\partial \theta}c_\theta N = \frac{S}{\sigma} \tag{1.1}$$

where $N(\sigma, \theta; x, y, t)$ is the action density as a function of intrinsic frequency (σ), direction (θ), horizontal coordinates ($xandy$), and time (t). The first term on the left is the local rate of change of action density in time, the second and third terms represent the propagation of action in space (with corresponding propagation velocities c_x and c_y in x and y space), the fourth term is the shifting of relative frequency as a result of varying depths and currents (with propagation velocity c_σ in σ space), the fifth term characterizes depth and current induced refraction (with propagation velocity c_θ in θ space), and the right hand side's term represents all the possible source/sink terms (Booij et al., 1999; Ris et al., 1999). These source terms are wind growth, nonlinear triplet and quadruplet wave-wave interactions, whitecapping, bottom friction, and depth-induced wave breaking. The SWAN model can use a structured or unstructured computational mesh.

Regional Tidal and Storm Surge Model

The hydrodynamic numerical model used for this study was ADCIRC, which is a two/three-dimensional unstructured finite element model capable of simulating tide, storm surge, and tidal velocities. The model solves the equations of motion for a moving fluid on a rotating earth, formulated using the traditional hydrostatic pressure and Boussinesq approximations, which have been discretized in space and time utilizing the finite element method and finite-difference method, respectively (Luettich et al., 1992). For this study, ADCIRC was run as a two-dimensional depth-integrated (2DDI) model that solves for water elevation based on the solution from the depth-integrated continuity equation from the General Wave Continuity Equation (GWCE), shown in Equation 1.2. The depth averaged velocities are obtained from the 2DDI momentum Equations 1.4 and 1.5. In both solutions all nonlinear terms have been retained (Luettich et al., 1992).

$$\frac{\partial^2 \zeta}{\partial t^2} + \tau_0 \frac{\partial \zeta}{\partial t} + \frac{\partial A_x}{\partial x} + \frac{\partial A_y}{\partial y} - UH\frac{\partial \tau_0}{\partial x} - VH\frac{\partial \tau_0}{\partial y} = 0 \tag{1.2}$$

where ζ is the surface water elevation, τ_0 is the spatially varying numerical weighting factor, and A_x, A_y are defined as follows:

$$\begin{aligned} A_x &\equiv \frac{\partial UH}{\partial t} + \tau_0 UH = \frac{\partial Q_x}{\partial t} + \tau_0 Q_x \\ A_y &\equiv \frac{\partial VH}{\partial t} + \tau_0 VH = \frac{\partial Q_y}{\partial t} + \tau_0 Q_y \end{aligned} \tag{1.3}$$

where H is the total water depth, U and V are the tidal velocity components, and Q_x and Q_y are the volumetric flux in x and y directions. The momentum equations can be written as:

$$\begin{aligned} \frac{\partial U}{\partial t} + U\frac{\partial U}{\partial x} + V\frac{\partial U}{\partial y} - fV = -\frac{\partial}{\partial x}\left[\frac{p_s}{\rho_0} + g\zeta - g(\eta - \gamma)\right] + \\ \frac{\tau_{sx}}{\rho_0 H} - \frac{\tau_{bx}}{\rho_0 H} + D_x - B_x \end{aligned} \tag{1.4}$$

$$\begin{aligned} \frac{\partial V}{\partial t} + U\frac{\partial V}{\partial x} + V\frac{\partial V}{\partial y} + fU = -\frac{\partial}{\partial y}\left[\frac{p_s}{\rho_0} + g\zeta - g(\eta - \gamma)\right] + \\ \frac{\tau_{sy}}{\rho_0 H} - \frac{\tau_{by}}{\rho_0 H} + D_y - B_y \end{aligned} \tag{1.5}$$

where f is the Coriolis parameter, p_s is the atmospheric pressure at the free surface, ρ_0 is the density of water, g is the gravitational acceleration, $(\eta - \gamma)$ represents Newtonian tidal potential, Earth tide, self-attraction, and load tide, (τ_{sx}, τ_{sy}) are applied free surface shear stresses, (τ_{bx}, τ_{by}) are bottom shear stresses, (B_x, B_y) are 2DDI baroclinic pressure gradients, and finally (D_x, D_y) are 2DDI momentum diffusion/dispersion terms (Luettich et al., 1992).

Coupled Wave-Surge Model

The coupling of wave and circulation models allows for the wave-current interactions, such as wave set-up and set-down, to be properly captured, resulting in more ac-

curate wave and storm surge outputs. In this study, the tightly coupled SWAN+ADCIRC model was implemented. At a given time step ADCIRC passes wind velocities, water levels, currents, and friction roughness lengths to SWAN, SWAN then uses this information to adjust its own computations (water depth and all wave related processes), and then sends the wave radiation stress gradients as a forcing function back to ADCIRC (Dietrich et al., 2011). The actual coupling of SWAN and ADICRC works because the two models can be carried out over the same unstructured computational mesh utilizing intra-core communication. In this coupled model, the computations are carried out in parallel, allowing for the global mesh to be decomposed and distributed over several computational cores. This minimizes inter-core communication due to the creation of local sub-meshes where the boundary node information is shared at the sub-mesh interfaces (Dietrich et al., 2011; Dietrich et al., 2012). A schematic of the way this coupled model communicates is shown in Figure 1.6. Another important aspect of this mesh decomposition is it allows for an increase in the computational speed.

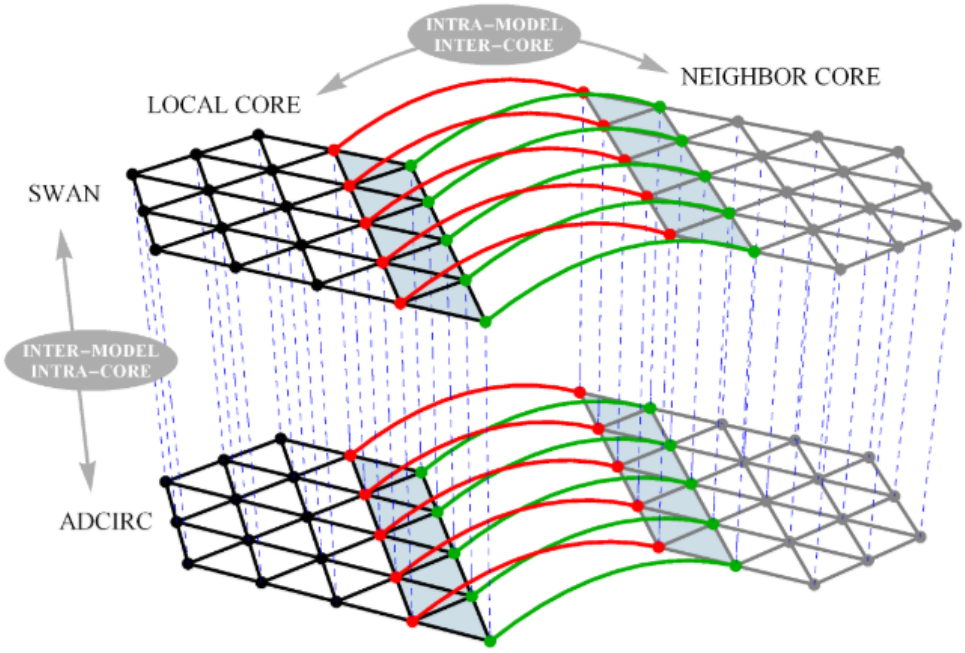

Fig. 1.6. Schematic of the coupled SWAN+ADCIRC parallel computational communication (Dietrich et al., 2011).

The computational domain for the SWAN+ADCIRC model used in this study was based on the NECOFS FVCOM GOM4 mesh, which has a total of 53,087 nodes and a resolution of 1 km along the Rhode Island coastline. The resolution for Rhode Island was increased to be around 200 m near the coast and approaches 20 m within the inlets, coastal ponds, and rivers (Torres et al., 2017). The model domain for this study is shown in Figure 1.7, with (a) showing the full regional model domain, (b) showing the increased resolution around Rhode Island, and (c) showing the Charlestown study area. Increasing the resolution for Rhode Island resulted in the full domain having a total of 105,560 nodes.

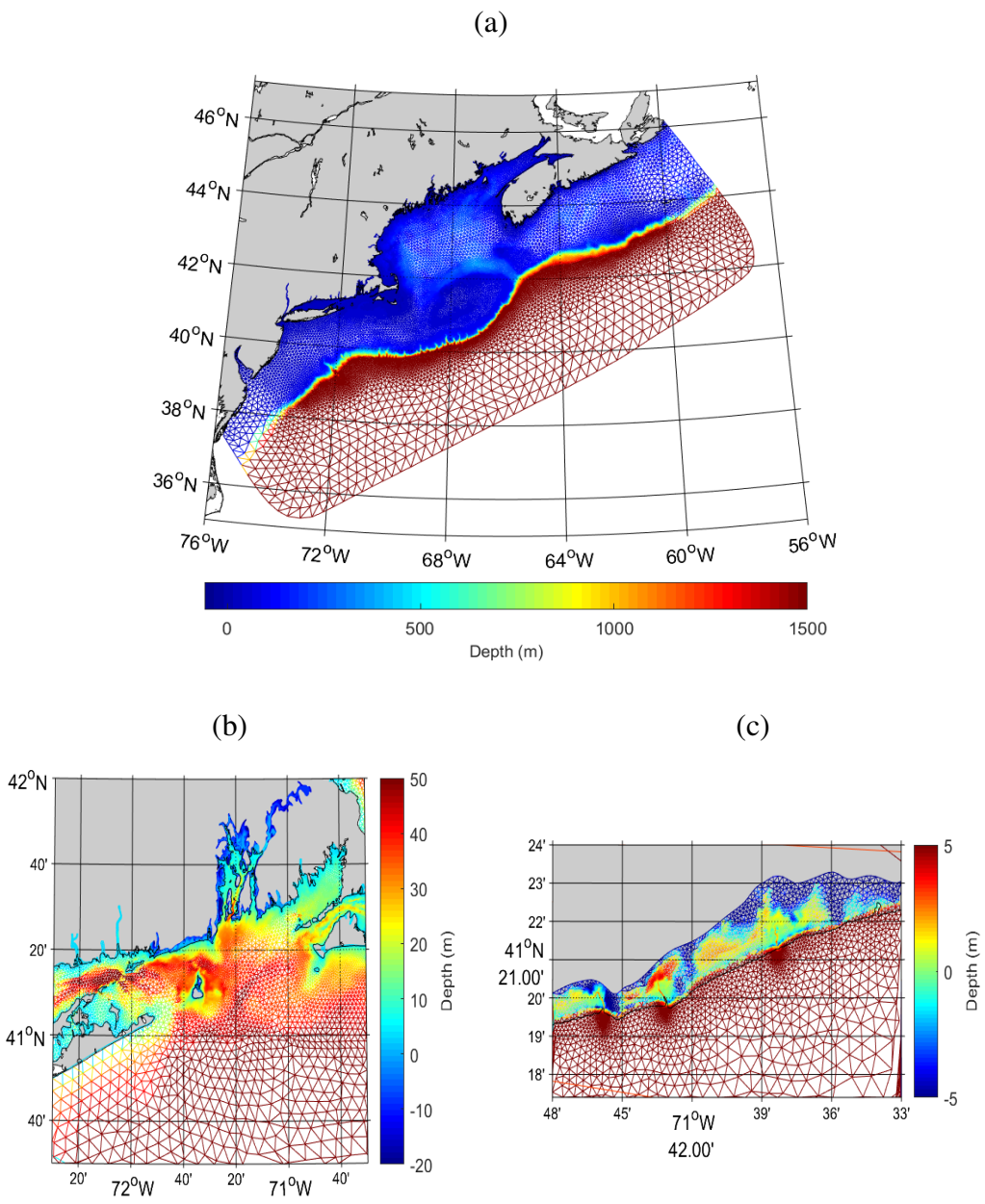

Fig. 1.7. Coupled SWAN+ADCIRC regional model domain. (a) Full regional model computational domain, (b) focus on the increased domain resolution in Rhode Island, and (c) zoomed in view of the domain for Charlestown.

STWAVE vs. SWAN

A comparison of the STeady-state specatral WAVE (STWAVE) model and SWAN model was made in this section for two reasons: (1) Previous risk assessment studies have used STWAVE for the wave climate, therefore it is important to compare the methodology

of this research to the previous ones, and (2) STWAVE and SWAN are both accepted for estimating offshore wave heights by FEMA, while for nearshore wave effects STWAVE is approved as opposed to SWAN (FEMA, 2018).

STWAVE is a steady-state, phase averaged, spectral wave transformation model based on the wave action balance equation. This model uses a wave action approach to handle currents as an energy spectrum approach cannot. The STWAVE model incorporates several physical processes. It simulations both depth-and current-induced wave refraction and shoaling, and includes many source/sink terms, which are: depth-and steepness-induced wave breaking, wind-induced wave growth, wave-wave interactions, and white-capping (Smith et al., 2001).

The SWAN model was already previously discussed in detail, and has many similarities to STWAVE. To summarize, SWAN is also a phase averaged wave model based on the spectral wave action balance. Like STWAVE, the SWAN model simulates both depth-and current-induced shoaling and refraction, and includes several source/sink term options: depth-induced breaking, wind-induced wave growth, wave-wave interactions (triplet or quadruplet), white-capping, and bottom friction. Unlike STWAVE, SWAN has the option to compute a time varying solution, rather than just a steady state one, and can be executed over an unstructured domain.

The two models were setup to compute over the same size structured domain using identical topo-bathy data, shown in Figure 1.8. The resolutions of the two model grids were created to be about the same, and SWAN was run in stationary mode so the models could be run utilizing the same basic inputs: significant wave height, peak period, swell direction, wind velocity, and wind direction. The basic inputs used for the two models are shown in Table 1.1. The swell direction and wind direction of 180° means propagation from the south towards shore.

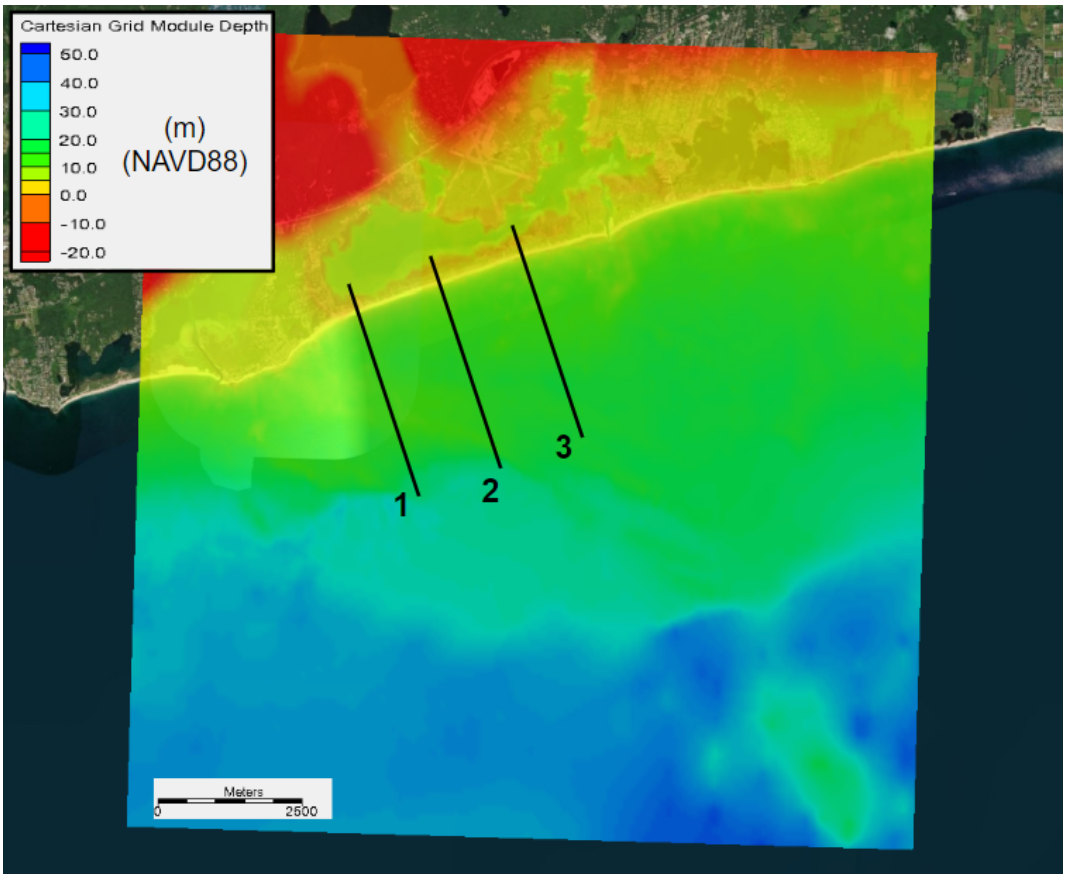

Fig. 1.8. Idealized domain in Charlestown, RI used for the comparison between the STWAVE and SWAN wave models. The location of the three transects used for the wave height comparison are shown. Note the grid shown is the STWAVE grid.

Table 1.1. Basic inputs for the STWAVE and SWAN comparison.

Hs (m)	Tp (s)	Wind Velocity (m/s)	Swell Direction (°)	Wind Direction (°)
6.0	20	20	180	180

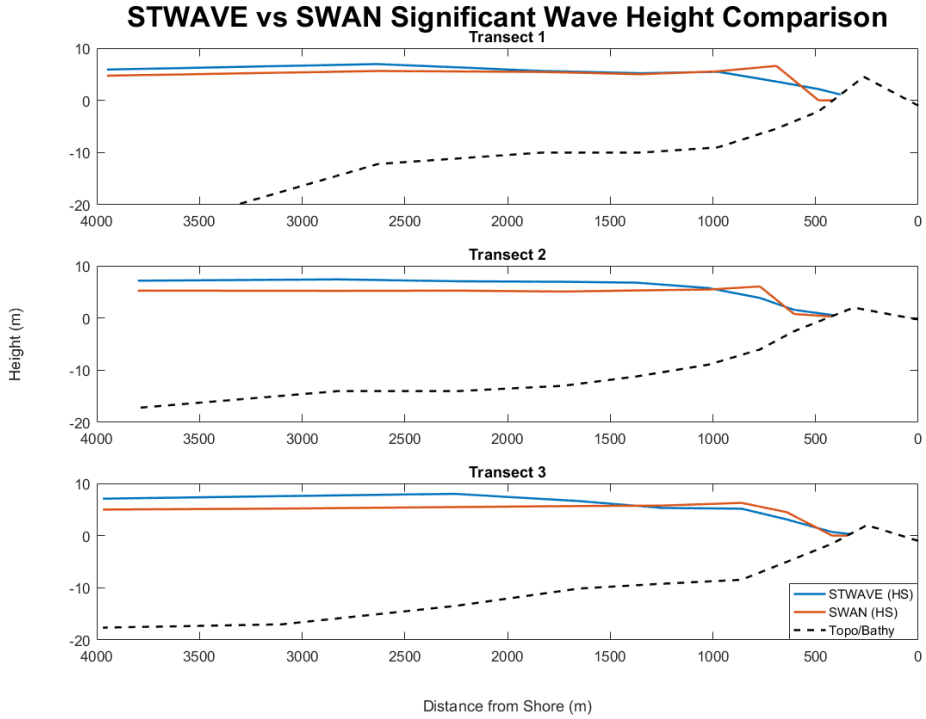

Fig. 1.9. Comparison of significant wave height between STWAVE and SWAN for the three transects in Charlestown, RI.

The significant wave height comparison between the two models is shown in Figure 1.9. The figure shows that in the offshore region STWAVE was typically predicting wave heights a meter or so larger. As the two models move into the nearshore region it switches, and SWAN begins to predict the larger wave heights. The best agreement in the nearshore region is shown in Transect 3, where the two models align well. Generally, the two models perform similar and predict wave heights relatively close to each other. However, it is important to keep in mind that the difference in wave heights of a meter can have a substantial impact when estimating damage to structures. These differences between the two model outputs are attributed to the fact that each model uses different governing equations to parameterize the source/sink terms, which can be found in each model's corresponding manuals (Booij et al., 1999; Smith et al., 2001). Generally, SWAN is considered the more advanced model and has also been extensively validated. It is also important to state that in this risk assessment, SWAN is not run in stationary mode,

which will improve the accuracy of the results. The results show reasonable correlation, but this was a simplistic comparison for the purposes of this study, further research is necessary to determine if SWAN should be FEMA approved for nearshore modeling.

1.2.3 Forecast System

This study also implements a coastal risk assessment forecast system for Rhode Island based on previous research (Hayward, 2017). The system was originally developed and tested by Hayward (2017), and was maintained and implemented throughout this study. Figure 1.10 shows a simplified flowchart for the forecast system. This system utilizes the same coupled SWAN+ADCIRC model and computational domain that was discussed in the previous section. It works by using a series of MATLAB and Bash scripts that download and pre-process the wind forcing, change the required input files, and then submits the files to begin the simulation. The system is run from a user desktop for the pre-processing, and then the input files are automatically moved to a High Performance Computing (HPC) cluster for the actual forecast simulations.

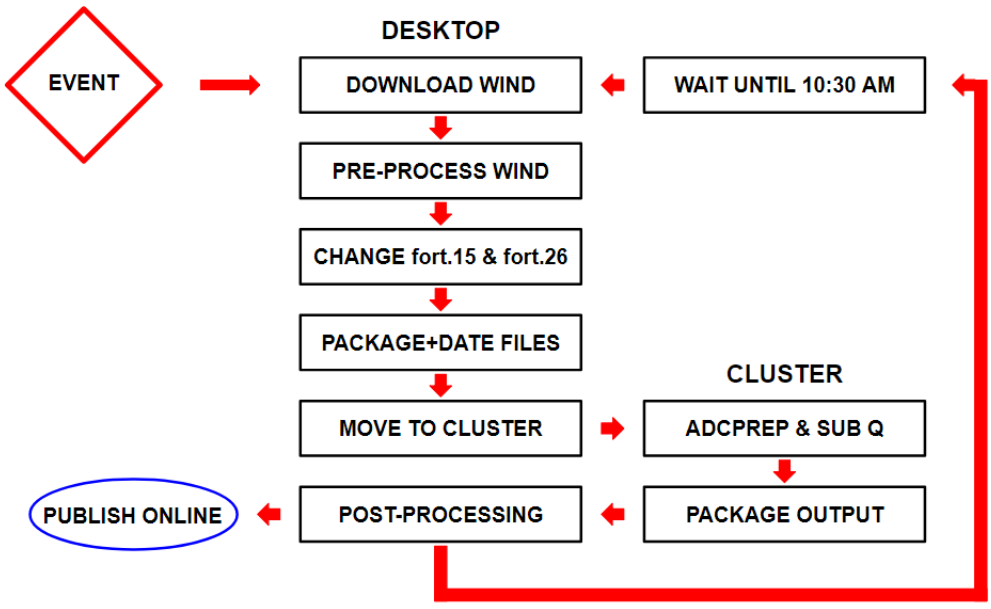

Fig. 1.10. Simplified flowchart for the SWAN+ADCIRC forecast system for Rhode Island coastal waters (Hayward, 2017).

In the current configuration of the system, it is setup to utilize the NECOFS WRF wind, which was shown to be the most accurate wind model for this area (Torres et al., 2017). The wind is downloaded as 3 days of hindcast data and 3 days of forecast data, resulting in a total simulation of 6 days. Currently, the forecast system runs on 64 processors allowing the simulation to be complete in just under 6 hours. This means that the model's forecast storm surge and wave height predictions can be made available for emergency planners, government officials, and the public 6 hours after a storm posing risk to Rhode Island is identified.

1.2.4 The North Atlantic Coast Comprehensive Study

Following the devastation caused by Hurricane Sandy, the USACE conducted the North Atlantic Coast Comprehensive Study (NACCS), with the goals of providing a risk management index for coastal areas, and to promote coastal resilient communities to both short and long term risks (USACE, 2015). Through the completion of this study damage functions were developed by analyzing the actual physical damage that occurred to structures in New York and New Jersey. These damage functions correspond to specific structure types that are typically found in coastal areas. The damage functions can assess the risk to a structure from inundation, wave attack, and erosion. In this study the inundation and wave attack damage functions were used, and the structures in the study area were classified according to the NACCS methodology.

This study also aimed to investigate the future risk to communities. NACCS investigated the threat from storms to the northeast U.S. by modeling the storm surge and wave heights of 1,050 synthetic tropical storms and 100 historical extra-tropical storms (USACE, 2015). The synthetic storms varied in magnitude, and some of the synthetic tropical storms modeled matched the 100-year return period storm surge water level in Newport, RI. Specifically, NACCS synthetic storm #492 was considered to represent a 100-year storm, which is defined as a storm that has a 1% annual chance of occurrence.

1.2.5 Structure Information and Classification

For this risk assessment model, it was necessary to have the geographic reference (Latitude and Longitude), and basic structural characteristics for every structure in the selected study area. The structures must be characterized in a method that remains internally consistent with the prototype classification for the damage functions. The prototype classification is shown in Table 1.2.

Table 1.2. USACE NACCS damage function prototype classification (USACE, 2015).

NACCS Prototypes	
Prototype Number	Prototype Description
1A-1	One-Story Apartment-No Basement
1A-3	Three-Story Apartment-No Basement
1B-1	One-Story Apartment-With Basement
1B-3	Three-Story Apartment-With Basement
2	Commercial-Engineered
3	Commercial-Pre/non Engineered
4A	Urban High Rise
4B	Beach High Rise
5A	Single-Story Residence, No Basement
5B	Two-Story Residence, No Basement
6A	Single-Story Residence, With Basement
6B	Two-Story Residence, With Basement
7A	Building with Open Pile Foundation
7B	Building with Enclosed Pile Foundation

Another aspect of the structural characteristics that must be known was the first Finished Floor Elevation (FFE), referring to the height above grade of the first floor for each structure. This information is vital to implementing the damage functions, as the damage calculations are very sensitive to this parameter. For example, a structure on stilts (7A or 7B) has a higher FFE than any other prototype, and therefore is the most resilient to the storm effects of inundation and waves. It is important to note however that the more elevated the structure the more vulnerable it becomes to wind damage. Typically the trade-off between elevating to minimize flood effects while increasing the wind effects is still worthwhile. A schematic of this relationship is shown in Figure 1.11.

As the figure shows, the structure that is elevated with the higher FFE is out of harms way in regards to flooding effects, while the structure that is not raised with a low FFE will be more affected by the flooding.

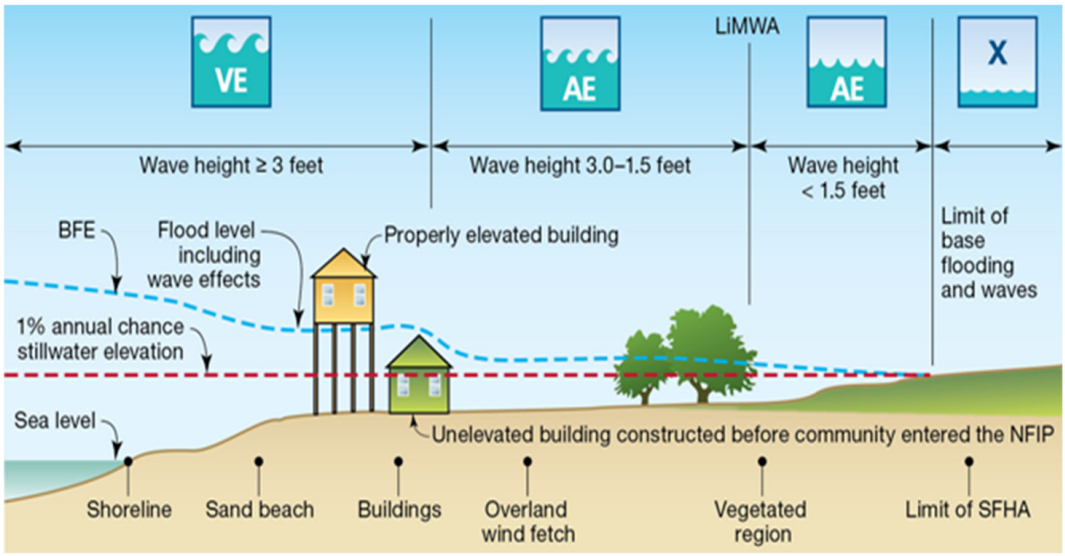

Fig. 1.11. FEMA diagram depicting the importance of elevated structures to increase resilience to storm effects of inundation and waves (FEMA, 2015). BFE stands for base flood elevation, and is the combination of the SWEL (still water elevation) and Wave Heights.

For the application to Charlestown, the geographic location for each structure was obtained from the emergency call data base (E911) that is available on a state-wide basis from the Rhode Island Geographic Information System (RIGIS) website (http://www.rigis.org/). In the selected study area a total of 1,323 structures were analyzed, which were determined based on the 100-year storm with 7 ft of SLR flood extent found on STORMSTOOLS (http://www.beachsamp.org/stormtools/). The necessary structural characteristics, including prototype classification and FFE were provided from a past study (Spaulding et al., 2016). The distribution of the structures by prototype throughout the study area is shown in Figure 1.12, and Table 1.3 shows the actual total of each prototype. As both the figure and table show, the prototypes found in the Charlestown study area are 5A, 6B, 7A, and 7B.

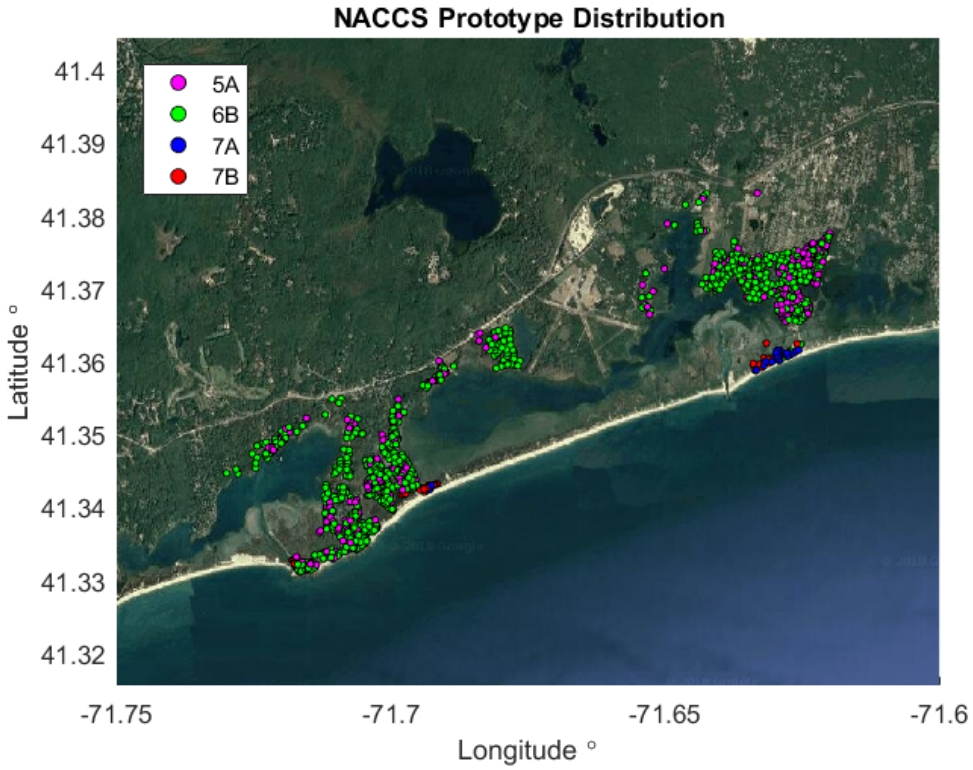

Fig. 1.12. Location and prototype distribution for every structure found in the Charlestown, RI study area.

Table 1.3. Total number of each NACCS prototype found in the study area.

Prototype	Description	Total Structures	Percent of Total (%)
5A	1 story, no basement	369	28
6B	2 story, basement	878	66
7A	Open Stilts	36	3
7B	Enclosed Stilts	40	3
	Total	**1,323**	

1.2.6 Damage Functions

As mentioned, NACCS developed damage functions that estimate structural damage as a function of inundation and waves. This study used slightly modified versions of the inundation and wave damage functions from NACCS to compute the structural damage estimates. The damage functions were based on the best curve fit to the NACCS data points to provide smoother damage curves. Each of the prototype classifications shown

in Table 1.2 have a corresponding damage function for inundation and wave damage. The damage functions work based on the flood depth level (ft) relative to FFE, and wave crest (ft) relative to FFE. An example of these damage functions is shown in Figure 1.13, where (a) is inundation damage and (b) is wave damage for prototype 5A (single-story, no basement). The dots represent the actual data points, while the dashed lines are the best curve fits. Each curve has a minimum, most likely, and maximum curve, which shows the high level of uncertainty in these damage functions. NACCS also has developed similar damage functions for content damage as well.

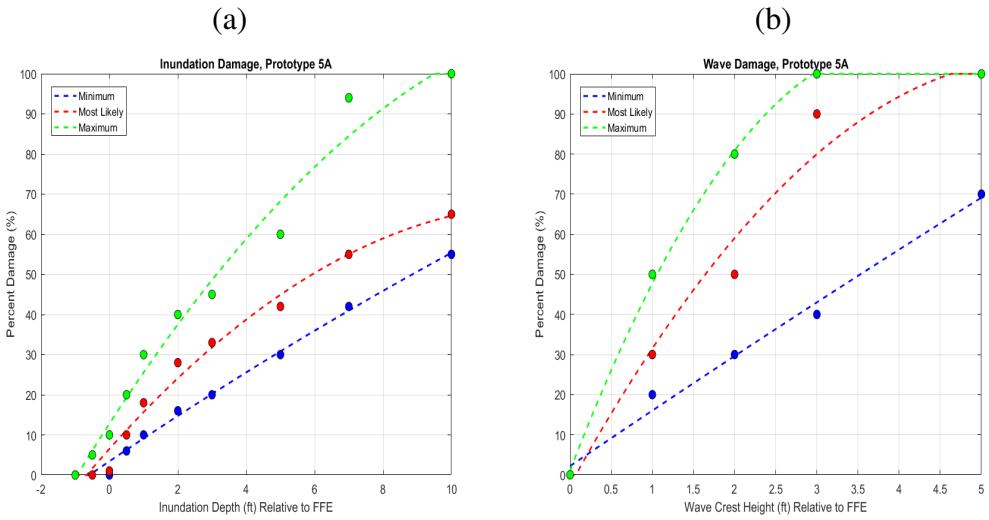

Fig. 1.13. NACCS damage curves for prototype 5A showing minimum, most likely, and maximum curves of damage. (a) Inundation Damage Curve and (b) Wave Damage Curve.

An integral part of these damage curves is the way the estimated damage to a structure changes depending on whether it has a basement or not, and whether the structure is elevated. This is shown in Figure 1.14, which shows three inundation damage functions: (a) 5B, two-story, no basement, (b) 6B, two-story, with basement, and (c) 7A, stilted structure. When a basement is present, the damage to the structure can begin below the FFE, meaning the water enters the basement and begins to cause damage. When a structure is elevated it becomes much more resilient to the damaged

produced by the storm effects.

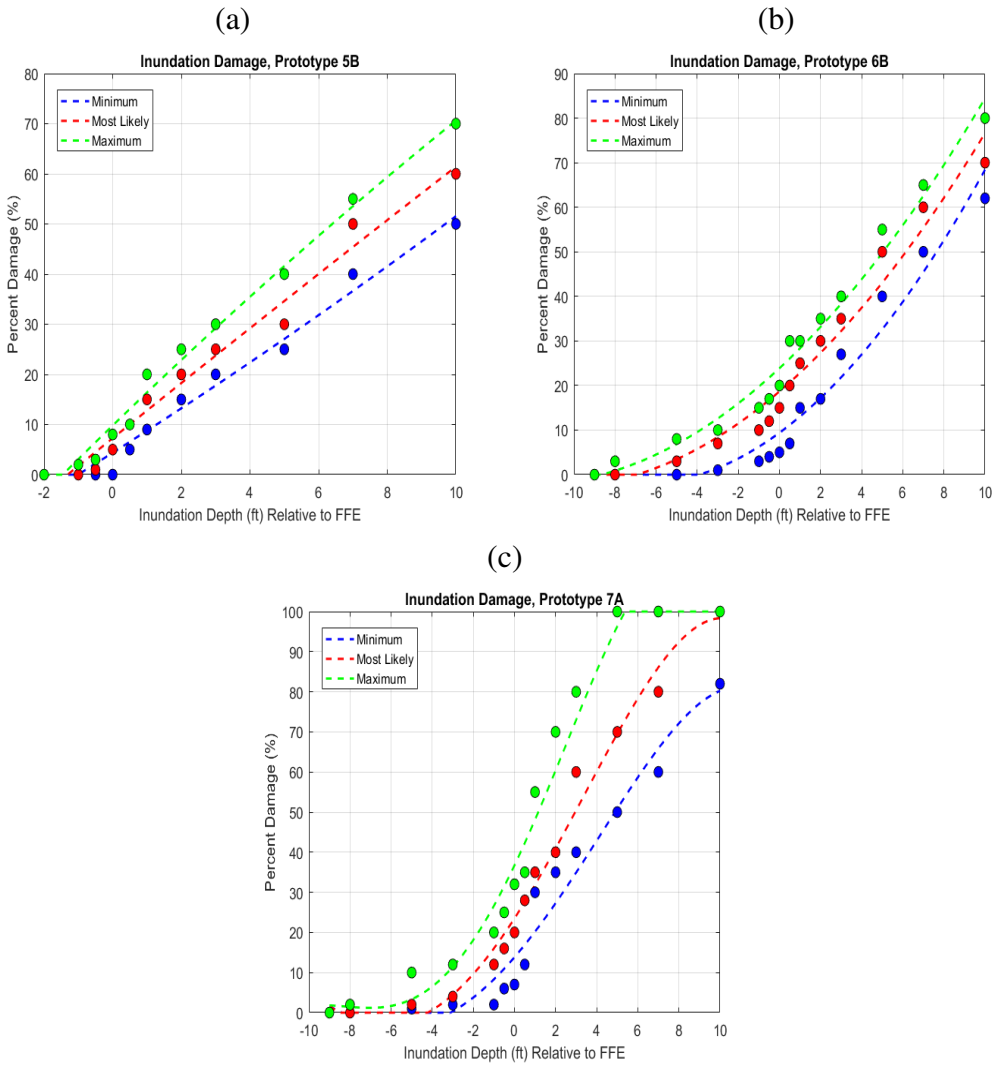

Fig. 1.14. NACCS damage curves for prototypes 5A, 5B, and 7A showing minimum, most likely, and maximum curves of damage. (a) Prototype 5B (no basement), (b) Prototype 6B (basement), and (c) Prototype 7A (open stilts).

1.2.7 Coastal Risk Assessment Model

This study implemented a Matlab based coastal risk assessment model. This model is compatible with the coupled SWAN+ADCIRC model outputs, and allows for the forecasting of structural damage to coastal communities. This coastal risk assessment tool requires the storm water levels and corresponding wave conditions, individual structure/infrastructure characteristics, and the NACCS damage functions. The outputs

are geographic damage maps displaying the expected total structural damage to individual structures. The damage for each structure is defined as the maximum damage between the calculated inundation and wave damage value, as outlined in the NACCS report (USACE, 2015).

The required water levels and wave conditions implemented into the integrated risk assessment model were extracted from the coupled SWAN+ADCIRC model simulations. This coupled model has been set up to output the maximum water levels and significant wave heights over the entire domain. These results are then interpolated onto each individual structure in the Charlestown study area to give every structure a specific georeferenced water level and wave height. Using the known FFE information for each structure in the study area, the inundation depth above/below the FEE was determined. This is the value that was utilized for the inundation damage functions. The required input for the wave damage functions is the controlling wave crest (η_c). The wave crest is defined as 0.7 times the controlling wave height (H_c), where this controlling wave height is 1.6 times the significant wave height (H_s) assuming a Rayleigh distribution (Grilli et al., 2017). To convert the model output of significant wave height to controlling wave crest Equation 1.6 was used. This calculated controlling wave crest was added to the storm surge levels, and was used to determine the wave crest height above/below the FFE for every structure. The effects of wave runup were not considered in this assessment to be internally consistent with the NACCS methodology.

$$\eta_c = 1.12 H_s \tag{1.6}$$

This coastal risk assessment tool also includes an additional option to add wind damage estimates. The methodology to include the wind damage was based on a previous study that discussed a Wind Protocol, which used the FEMA Hazus hurricane loss model's fragility curves, along with structural characteristics, surface roughness,

and a determined wind gust speed (Bianchi et al., 2017). These fragility curves assess probability of damage due to a given wind speed based on the aforementioned inputs.

In order to implement the fragility curves for wind damage, the following structural characteristics must be known: number of stories, roof type, sheathing nail sizes, wall type, and the use of hurricane straps versus toe-nails. Most of this information can be derived from the Charlestown GIS database, but requires the user to identify and note each individual structure's information. For this study it was deemed unrealistic to manually click to identify all 1,323 structures' information, so the worst case scenario of the inputs was assumed. This corresponded to a two story gable roofed structure with wood frame, toe-nail strapping, and 6d sheathing (Bianchi et al., 2017).

The next required input was the surface roughness at each structure, which determines the corresponding vertical wind profile. These surface roughness values were based on the land use, and were provided by other research on a 30 m by 30 m grid for all of Rhode Island (Grilli et al., 2012). The values vary between 0.01 m and 0.73 m, and were then interpolated onto each structure in the study area. The next step was to bin these surface roughness values according to the four values FEMA uses for their fragility curves, which is shown in Table 1.4. The study area did not contain any urban development so no structures were binned into this 1.0 m category shown in the table. The wind forcing experienced by structures in high density suburban or urban areas is much lower than those structures that are located in relatively unobstructed regions, such as the open terrain.

Table 1.4. FEMA Hazus wind fragility curve surface roughness values based on land use (FEMA, 2012).

Land Use Category	Roughness Length (m)
Open Terrain	0.03
Suburban	0.35
Suburban High Density	0.70
Urban	1.00

The final required input was the wind speed (in mph) that will be used to determine probability of damage from the fragility curves. If the storm being simulated by the coupled regional model has strong enough wind speeds (> 60 mph) then the model's wind can be used. In the event that the simulated wind speed does not exceed this threshold the information is found through the Applied Technology Council (ATC) website. ATC publishes wind speed by location in accordance with the American Society of Civil Engineers (ASCE) determination of design wind loads for structures. On this website it is easy to find the wind speed for a selected area, and it provides an estimate for the 10, 25, 50, 100, 300, and 700 year return interval wind speed.

With the structural characteristics assumed, the surface roughness at each structure known, and the wind speed for the region determined the fragility curves were implemented. An example fragility curve is shown in Figure 1.15. As the figure shows there are four different curves, which correspond to the four different damage states where the assumed damage percentages are 10%, 30%, 60%, and 100%. The shown classification also has fragility curves for surface roughness values of 0.35 m and 0.7 m.

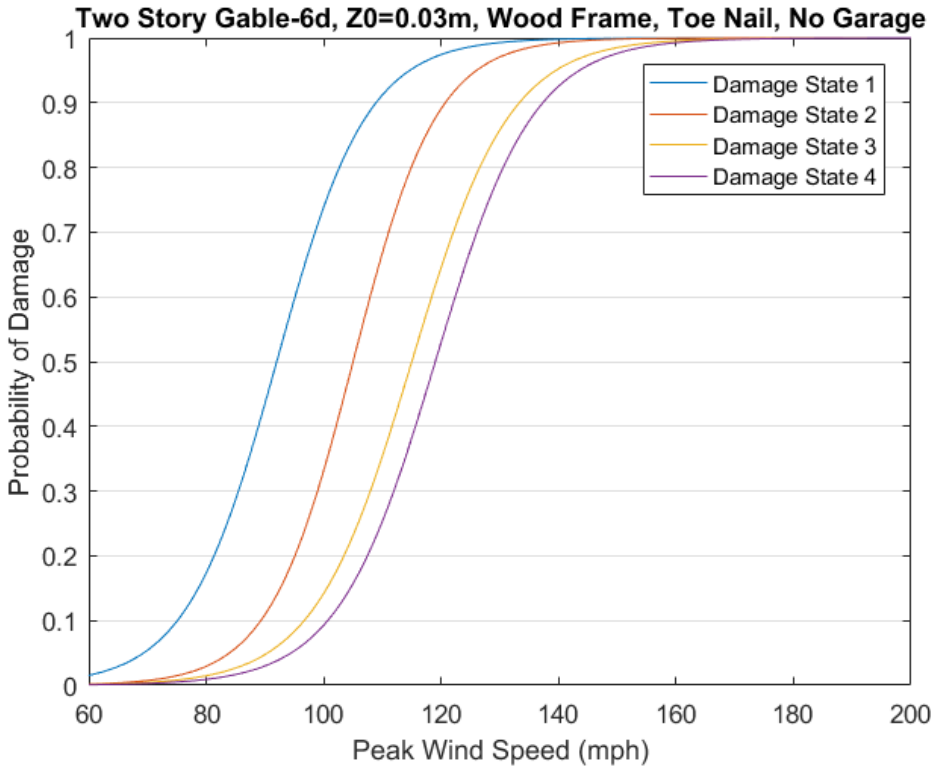

Fig. 1.15. FEMA Hazus wind fragility curve for a two-story gable roofed structure with wood frame, toe-nail strapping, and 6d sheathing (FEMA, 2012).

A weighted damage calculation method was implemented to determine an actual damage percentage for each structure. The equation used for this calculation is shown in Equation 1.7, which multiples the assumed damage for each damage state with the probability of each respective state at a given wind speed (Bianchi et al., 2017). The products are then added and normalized over the summation of the assumed wind damage percentages.

$$D_w = \frac{\sum(DS * P) - 4}{200\%} \tag{1.7}$$

where D_w is the resulting wind damage as a percentage, DS refers to the four different assumed damage state percentages, P is the associated damage probability for the specific damage state, and 200% is the sum of all the assumed wind damage state

percentages.

Once the damage from storm surge, waves, and wind are calculated separately the total damage is set to be the maximum value between all three, shown by Equation 1.8.

$$D_T = max(D_s, D_{wa}, D_w) \tag{1.8}$$

where D_T is the total damage, D_s is the surge damage, D_{wa} is the wave damage, and D_w is the wind damage.

1.2.8 Storms of Interest and Validation

This section will discuss the storms that were selected for the coastal risk assessment, as well as the validation for the coupled SWAN+ADCIRC model for these storms. The simulations were performed for both historical and future storms. The historical storm that was selected as primary importance was Hurricane Sandy due to its recent impact, and the availability of the NECOFS WRF wind data. Large winter storms, also known as Nor'easters, were simulated in forecast mode and validated. However, these storms produced little damage to the study area, and for this reason a hypothetical future storm that would result in damage was used from the NACCS storm database. Both the Hurricane Sandy and NACCS storm wind speeds did not exceed the 60 mph threshold in the study area for the calculation of wind damage. In this risk assessment the 100-year return wind speed was derived from the ATC website, and used for the wind damage calculations. The damage was initially calculated just from the effects of storm surge and wave attack, with the wind damage kept separate.

Hurricane Sandy occurred in late October 2012. When it made landfall in New Jersey it was only a post-tropical cyclone, but was such a large storm in terms of radius of maximum wind that it had strong surge impacts to the whole Northeast. The track of Hurricane Sandy is shown in Figure 1.16. The combination of the storm surge and wave heights from this storm produced damage to the southern coastal communities of Rhode

Island. In many areas the dunes were fully eroded leading to over-topping, allowing the storm effects to propagate further inland.

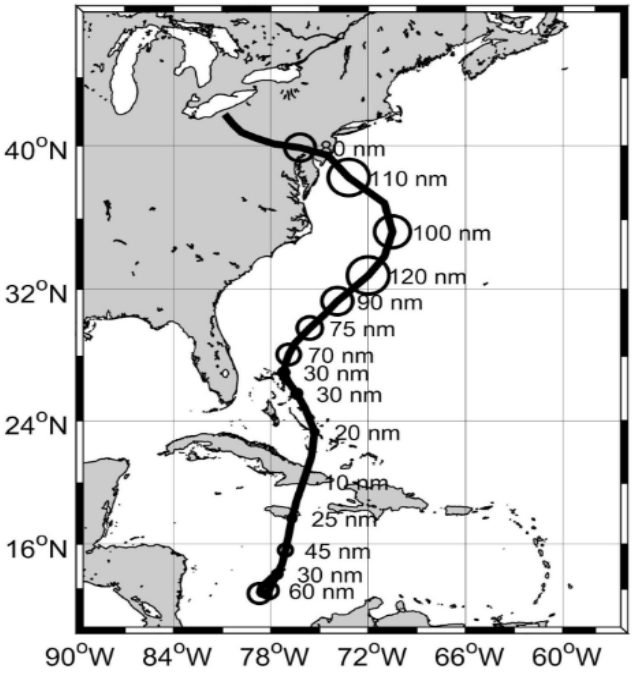

Fig. 1.16. Hurricane Sandy track including radius of maximum wind in nautical miles (nm).

To ensure that the coupled SWAN+ADCIRC model was accurately simulating storm surge and wave heights a model validation was performed. For this study the validation was done by extracting NOAA recorded time series for water levels and wave heights at certain locations, shown in Figure 1.17. There were two tidal gauge stations used in this region: Newport (8452660) and Providence (8454000). The wave buoy used is located to the southeast of Block Island (Station 44097). The validation for Hurricane Sandy's water level and wave heights is shown in Figure 1.18. The coupled model performs well in simulating the water level at both locations, but has an issue at the beginning of the simulation. This can be attributed to the ramp function used in the model as it takes the model time to bring the tides up to phase. The model tends to underpredict the water levels slightly at both locations, but accurately captures the peak surge values. The Root

Mean Square Error (RMSE) values were 0.21 m at Newport and 0.24 m at Providence. The difference between the recorded and modeled peak water level is shown in Table 1.5, with both locations within 0.20 m of the observed value. Computed and observed wave heights were also compared. There was a discrepancy at the beginning of the simulation. This likely due to either the ramp function taking time to get the simulation up to speed or issues in the initial wind data, but regardless it estimates the timing and peak of the wave heights accurately. The RMSE for the significant wave height was 0.93 m for the entire simulations, which improves to 0.57 m when the error in the initial stage of the simulation was ignored. Table 1.5 shows that the difference between the modeled peak significant wave height and the observed was 0.08m. Even with the small discrepancies that were present it can be concluded that the model is performing well as it is reasonably close to the recorded values, and captured the timing of the storm correctly.

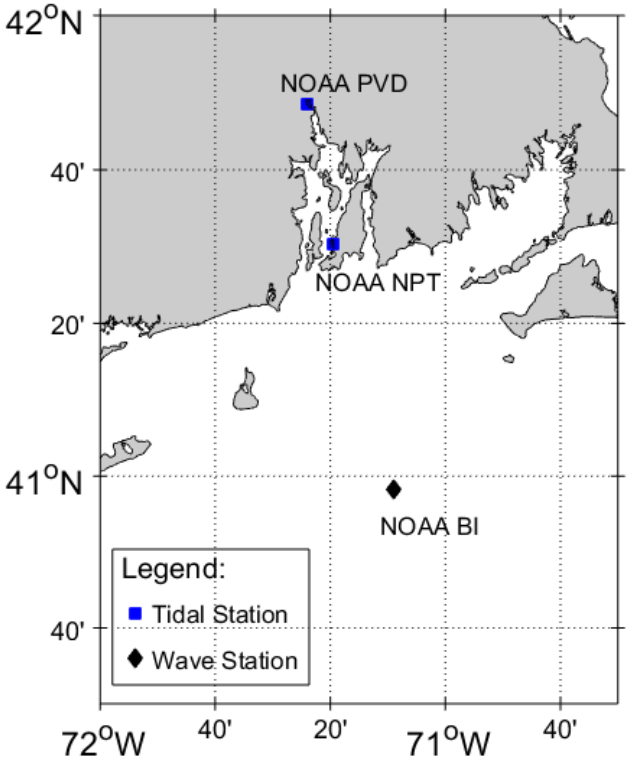

Fig. 1.17. Location of tidal and wave stations for model validation in Rhode Island. NOAA PVD is the Providence (8454000) tidal station, NOAA NPT is the Newport (8452600) tidal station, and NOAA BI is the wave station (44097).

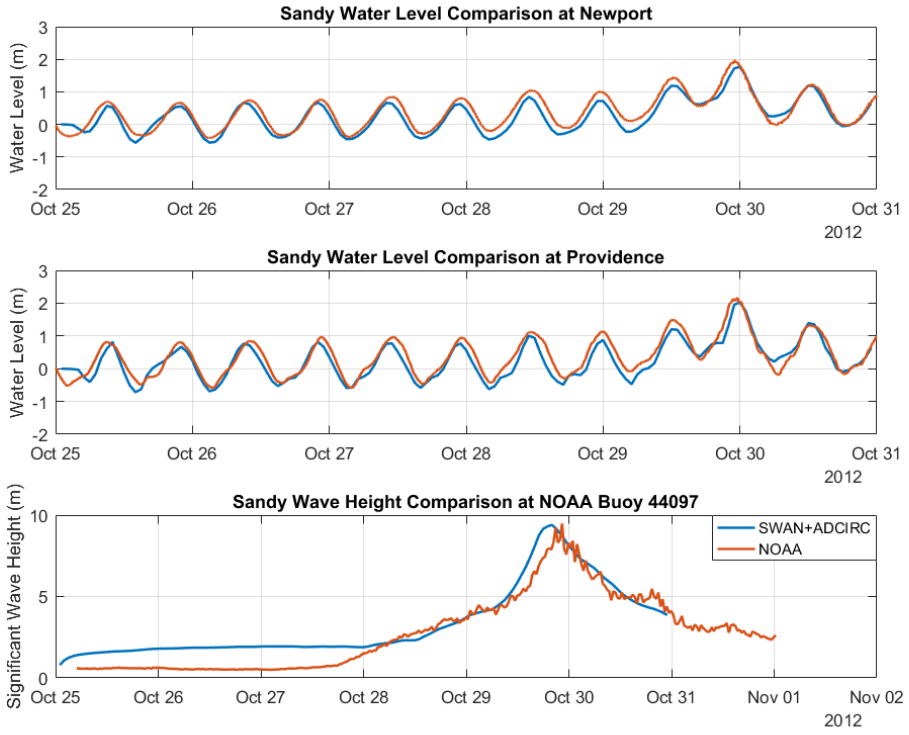

Fig. 1.18. Coupled SWAN+ADCIRC model validation for Hurricane Sandy water level at Newport and Providence tidal stations, and for significant wave height at Block Island wave station. The corresponding RMSE values were 0.21 m, 0.24 m, and 0.93 m, respectively.

Table 1.5. Hurricane Sandy modeled and recorded peak value comparison.

Water Level				
Station	Modeled (m)	Recorded (m)	Difference (m)	Error (%)
Newport	1.80	1.96	0.16	8
Providence	2.02	2.17	0.15	7
Significant Wave Height				
Station	Modeled (m)	Recorded (m)	Difference (m)	Error (%)
Block Island	9.40	9.48	0.08	1

During the period of this study two large Nor'easters occurred for the region that were used to test the forecast system. The first event was Nor'easter Stella, which was the most significant extratropical storm event of 2017, with the peak of the storm occurring on March 15th for Rhode Island. This storm produced levels of coastal flooding in New

Jersey and brought snowfall totals between 3 to 5 ft to areas across the Northeast. The second event was Nor'easter Riley, which was the largest and most damaging extratropical storm event of 2018 at the time of this report. The peak of this storm occurred on March 3rd for Rhode Island. Like Nor'easter Stella, this storm produced large quantities of snow, but the coastal flooding was much greater in comparison. The coastal flooding from this storm resulted in damage to parts of Massachusetts, New Jersey, and New York. In both cases, the forecast system was run before the expected peak of the storm to test the systems ability to properly forecast the maximum storm surge and wave heights. The results of the forecast simulations for these storms are shown in Figure 1.19 and 1.20, respectively.

The first validation for Nor'easter Stella shows good agreement between the model results and the observed data for both water levels and wave heights. In this forecast simulation, the RMSE value for water level was 0.16 m and was 0.58 m for significant wave height. The peak value comparison between modeled and observed values is shown in Table 1.6. The modeled peak surge value had an error of 12% and the peak significant wave height value had an error of 10%. Towards the end of the forecast period for the wave heights the system underpredicts the peak by about a meter, and continues to underpredict by a meter for the rest of the simulation. For the Nor'easter Riley simulation, the water level for was predicted well at both Newport and Providence with RMSE values of 0.23 m 0.32 m, and the significant wave height matched observations well at the initial stages of the simulation with a RMSE value of 0.92 m. The significant wave height in the forecast period was overpredicted by approximately a meter.

For the peak value comparison, the water levels had an error of 2% and 3% at Newport and Providence, and the significant wave height had a peak error of 1%, all shown in Table 1.7. These results show a noticeable error that occurs around March 3rd causing the water level to behave unexpectedly, and the wave heights around the peak

of the storm to be underestimated. The discrepancy was most significant in the wave height results, and it is likely that the issue causing these errors was in the wind data. To investigate if this was the reason, forecast wave height simulations that were performed on March 2nd and March 5th were further analyzed, shown in Figure 1.21. Both forecast system wave height results align much better with observations, capturing the ramp up to the storm peak and the actual peak of the storm well. Towards the tail-end of the storm both simulations tend to overpredict the wave heights by around a meter again. The RMSE values for these wave height results were 0.85 m and 0.80 m, and had peak errors of 13% and 15%. It was concluded that there was an issue in the wind data for the period of largest error in the previous simulation run on March 3rd, Figure 1.20.

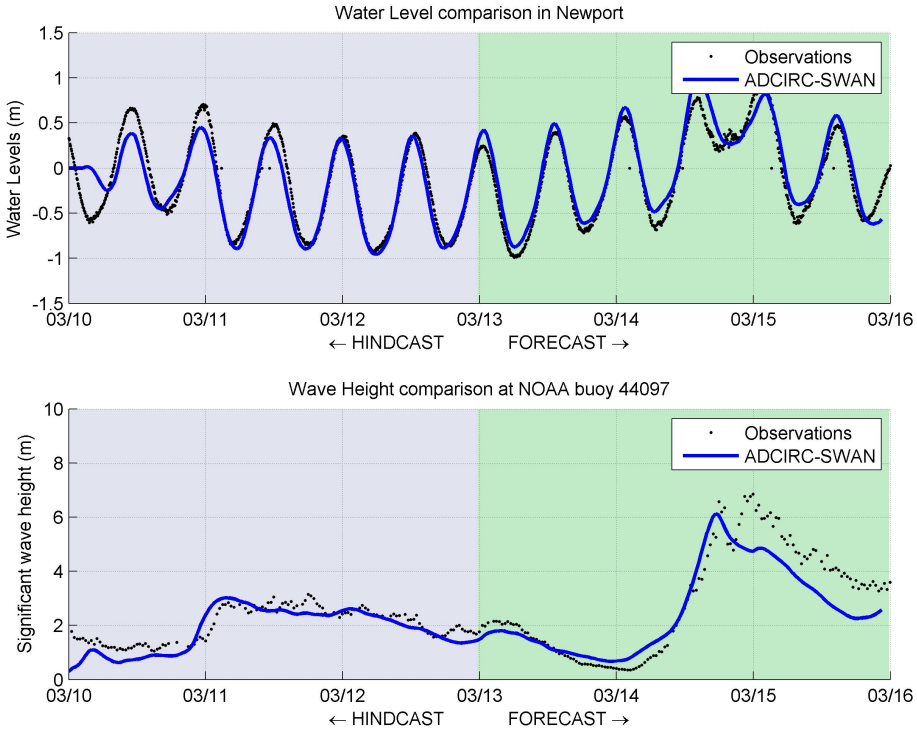

Fig. 1.19. Comparison of Winter Storm Stella forecast system results to observed water levels at the Newport tidal station and to significant wave heights at the Block Island wave station. For this forecast simulation, the RMSE values were 0.16 m at Newport and 0.58 m at Block Island. The blue region denotes the hindcast period and the green region denotes the forecast period. This simulation was run on March 13, 2017 (Hayward, 2017).

Table 1.6. Nor'easter Stella modeled and recorded peak value comparison.

Water Level				
Station	Modeled (m)	Recorded (m)	Difference (m)	Error (%)
Newport	0.87	0.99	0.12	12
Significant Wave Height				
Station	Modeled (m)	Recorded (m)	Difference (m)	Error (%)
Block Island	6.22	6.90	0.68	10

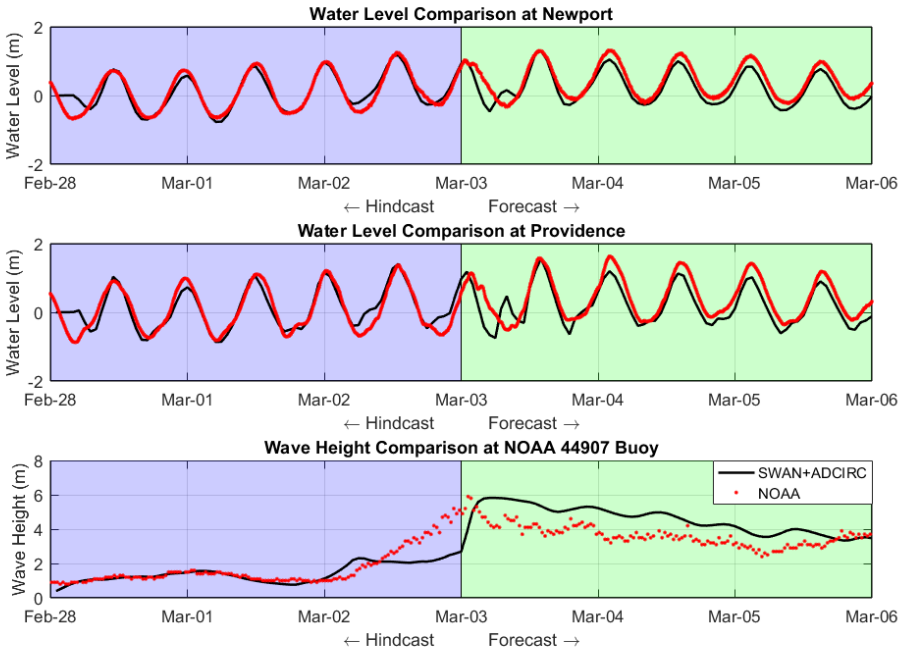

Fig. 1.20. Comparison of Winter Storm Riley forecast system results to observed water levels at the Newport and Providence tidal stations, and to significant wave heights at the Block Island wave station. For this forecast simulation, the RMSE values were 0.32 m, 0.23 m, and 0.92 m, respectively. The blue region denotes the hindcast period and the green region denotes the forecast period. This simulation was run on March 3, 2018.

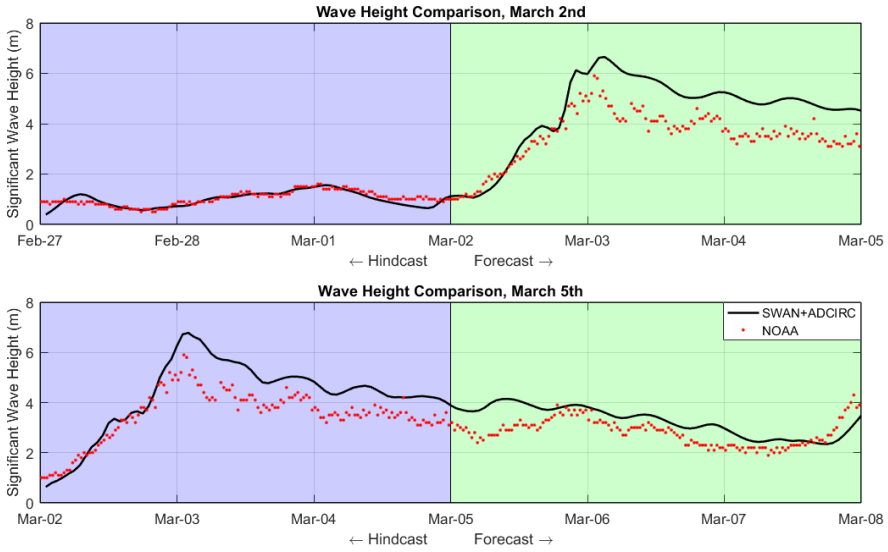

Fig. 1.21. Comparison of Winter Storm Riley forecast system significant wave height results to observed significant wave heights at the Block Island wave station. The top simulation was run on March 2, 2018, and had an RMSE of 0.85 m. The bottom simulation was run on March 5, 2018, and had an RMSE of 0.80 m. The blue region denotes the hindcast period and the green region denotes the forecast period.

Table 1.7. Nor'easter Riley modeled and recorded peak value comparison.

Water Level				
Station	Modeled (m)	Recorded (m)	Difference (m)	Error (%)
Newport	1.29	1.31	0.02	2
Providence	1.56	1.60	0.04	3
Significant Wave Height				
Run Date	Modeled (m)	Recorded (m)	Difference (m)	Error (%)
March 2nd	6.65	5.90	0.75	13
March 3rd	5.82	5.90	0.08	1
March 5th	6.78	5.90	0.88	15

These winter storms were useful in testing the forecast systems ability to accurately forecast the storm surge and wave heights in real-time. However, because these winter storms did not produce significant damage to the study area they were not implemented into the risk assessment system for this study. Instead a synthetic storm from the NACCS study was used as a 100-year storm for the study area. The synthetic storm

selected was storm #492, which had a storm surge around 2.0 m greater at Newport than either Nor'easter. The track for this storm including radius of maximum wind is shown in Figure 1.22. This synthetic storm was chosen because its peak storm surge value in Newport, RI closely matched the NOAA upper 95% confidence interval annual exceedance probability curve for the 100-year return period storm surge level for Newport. This NOAA curve for Newport is shown in Figure 1.23. The blue circle on the figure marks the water level value for the upper 95% interval, which is 2.80 m referenced to Mean Higher High Water (MHHW). This converts to 3.35 m referenced to NAVD88, and can be directly compared to the synthetic storm water level of 3.27 m (NAVD88), which shows a close correlation in values. This synthetic storm produces a water level of 2.89 m in Charleston, a difference of 0.38 m from the Newport value.

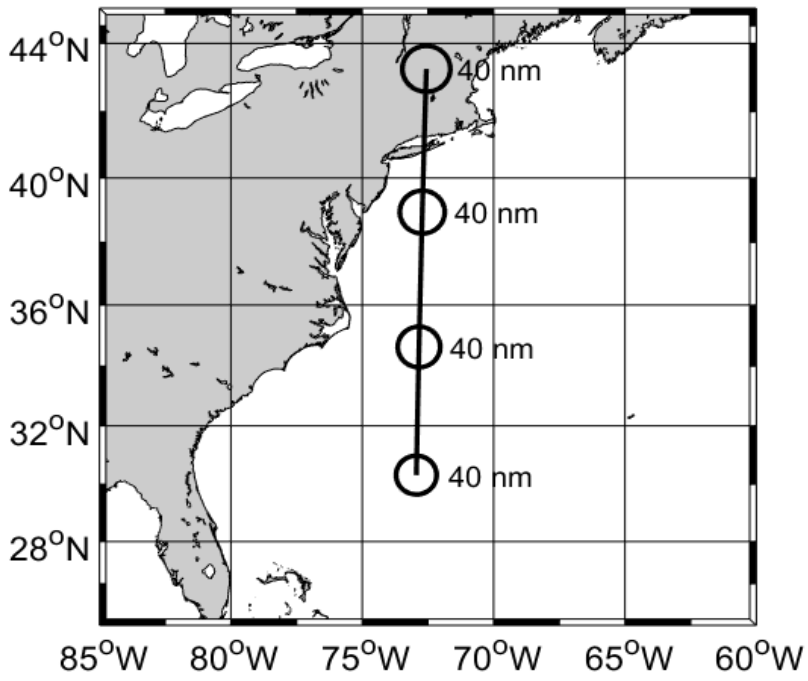

Fig. 1.22. NACCS synthetic storm #492 track including radius of maximum wind in nautical miles (nm). The forward motion of this storm was 60 mph.

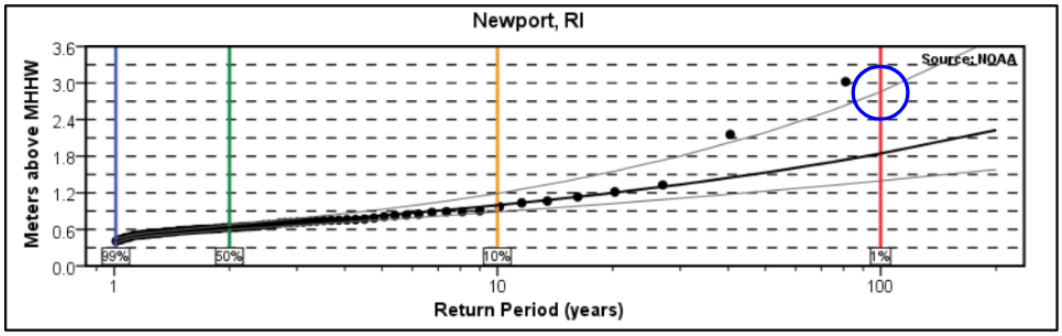

Fig. 1.23. NOAA annual exceedance probability curve for their Newport, RI tidal gauge station. The mean value is shown by the bold black line and the upper/ lower 95% confidence values are shown by the lighter black lines. The blue circle denotes upper 95% confidence interval value for the 1% annual water level (NOAA, 2013).

The water level output for the regional model for the synthetic 100-year storm was compared to NACCS save point data at Newport and Charlestown for this storm. This is shown in Figure 1.24, which shows a close correlation at both save point locations. The difference between the regional model and the NACCS save point data at Newport was 0.17 m and at Charlestown was 0.25 m. At the beginning of the simulation comparison a notable difference can be seen, which is a result of the regional model simulation including the effects of tides. This comparison was performed to ensure the regional model was capable of properly simulating the NACCS storm.

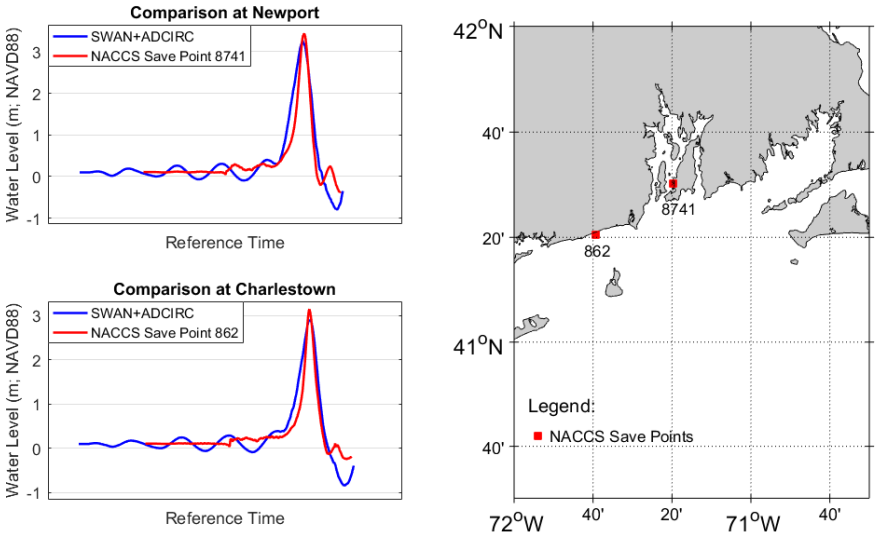

Fig. 1.24. Water level comparison of the regional model outputs for the synthetic 100-year storm to save points for NACCS storm #492 simulation outputs at Newport and Charlestown.

In the event of large tropical storms there is a high likelihood of dune erosion. This was made evident during Hurricane Sandy when many dune systems were over-topped. Numerical models have been developed that attempt to capture this erosion during the simulation. XBeach is an example of a sediment transport model that analyzes beach erosion. It is a fully integrated sediment transport model comprised of several modules: short wave, hydrodynamic and long wave, sediment transport, and morphologic (Roelvink et al., 2009). It can be forced with results from a coupled SWAN+ADCIRC model, and was shown to perform well in Charlestown, RI (Schambach et al., 2018). However, this XBeach model is very computationally expensive, and would be impractical to implement in this risk assessment system for this reason.

Instead, a modified eroded dune profile was added into the regional model for the Charlestown study area. This profile was loosely based on the 100-year storm dune profile developed by Brian Oakley, found in his technical report (Oakley, 2016). The term loosely was used because the coupled model works over an unstructured grid, which

does not guarantee nodes to be placed on/behind the dune system to fully capture the profile. For future studies this is one of the areas that could be improved by redeveloping the model domain to fully represent the dune profile. An example cross-section for this 100-year dune profile for Charlestown is shown in Figure 1.25. The figure shows that the peak dune elevation is decreased by roughly 2 m and the dune is flattened backwards into the coastal pond/marsh areas. This reduction in dune elevation allows stronger storm effects to propagate inland.

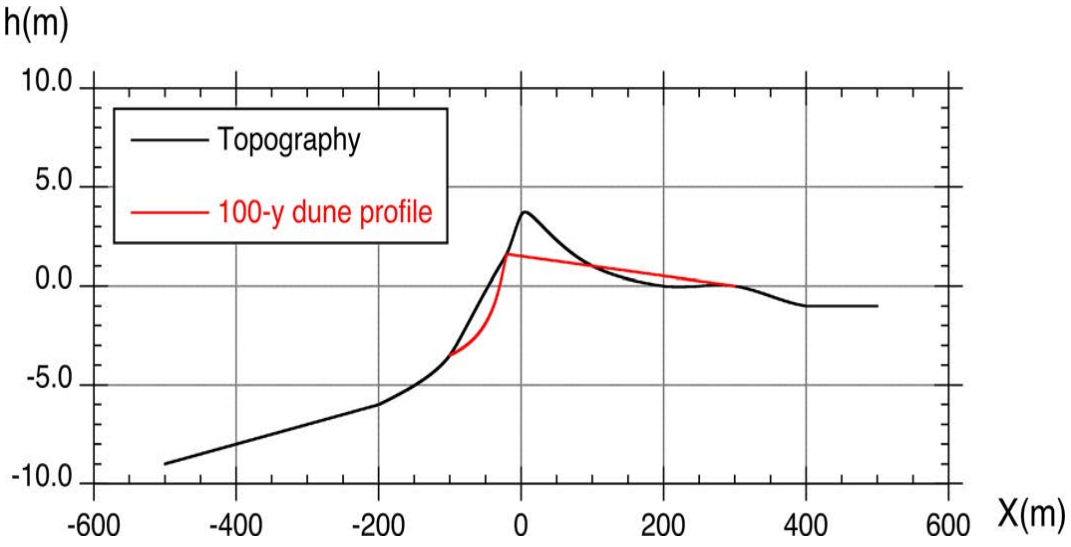

Fig. 1.25. Cross-section of the 100-year storm dune profile in Charlestown. Shows dune height (h) versus shore distance (X), vertically referenced to NAVD88 (Grilli et al., 2017).

Figure 1.26 shows the difference between the dune intact and dune eroded digital elevation models (DEM) used for the regional model in the study area. Areas marked by the orange and red colors show locations where the dunes were higher in the intact case, and the blue colors show areas that were higher in the dune eroded case. This means that the bright colors are the locations where the dunes were eroded and flattened backwards to fill in the blue areas for the dune eroded DEM, which is consistent with the cross-section profile shown in Figure 1.25.

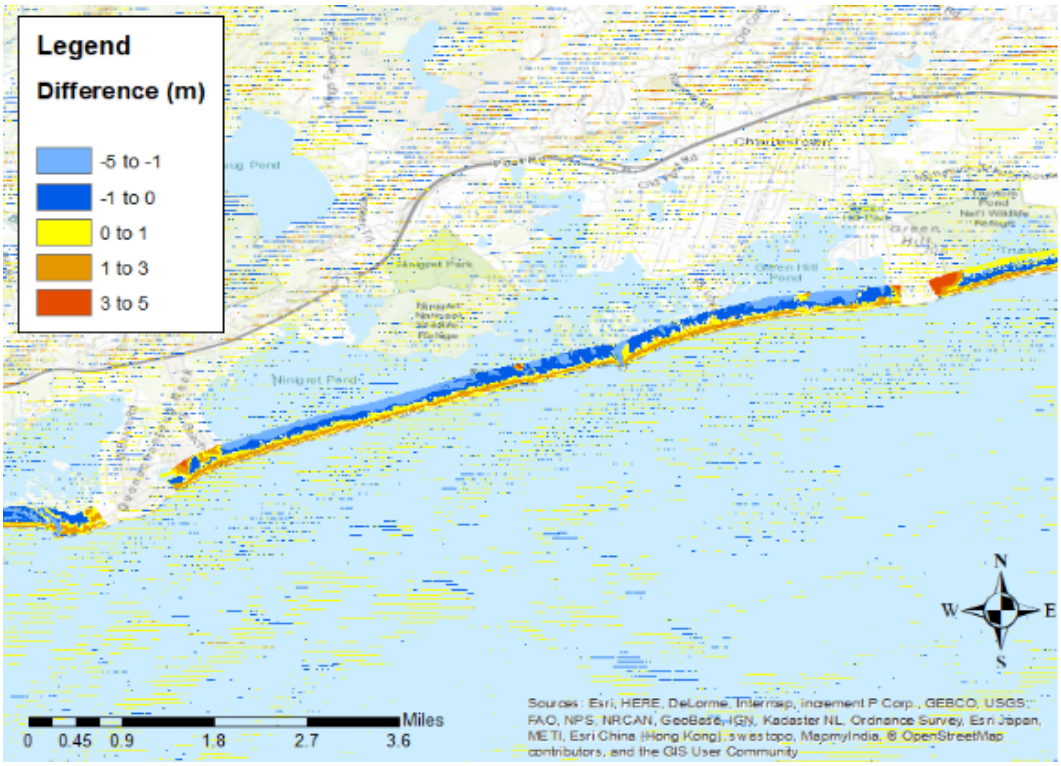

Fig. 1.26. Difference between the dune intact and dune eroded DEMs focused on Charlestown.

The simulations that were performed for the risk assessment were Hurricane Sandy and a synthetic 100-year storm, and in both cases simulations were performed with the dunes intact as well as with the dunes eroded. The same dune eroded profile was assumed for Hurricane Sandy to allow for a worst case scenario for the storm. Unfortunately, neither storm had a wind speed in the study area greater than the 60 mph wind fragility curve cut-off. To include wind damage, it was calculated using the published 100-year wind speed from the ATC website. The wind damage calculation was originally kept separate from the other damage calculations for the synthetic 100-year storm (i.e. storm surge and wave attack). This was done since the synthetic 100-year storm that was used did not have large enough wind speeds to result in damage. As a worst case scenario, the the 100-year storm surge event was coupled with the 100-year wind speed event with the eroded dune profile. It should be noted that this could also have been done for Hurricane

Sandy (a 25-year storm surge event) by coupling it with the 25-year wind speed event. In this scenario the wind speed did not produce any damage to the study area, so it was ignored.

An important assumption that was made in these storms was that the 100-year wave event occurred with the 100-year storm surge event. To add validation to this assumption, Wave Information Studies (WIS) stations in the regional model domain were investigated. These stations have published 100-year wave event values based on an extreme analysis of 35 years worth of wave data. Four stations located near Block Island were selected, and the corresponding values were compared to the coupled SWAN+ADCIRC model's significant wave height results for the synthetic 100-year storm. This comparison is shown in Table 1.8. The error between the WIS station values and the modeled values were all below 6%, and within 0.7 m of each other. This close correlation allows for the conclusion that assuming the 100-year storm surge event and 100-year wave event occur simultaneously was reasonable in this case.

Table 1.8. Comparison of the 100-year wave event value between WIS stations and the coupled SWAN+ADCIRC model.

Water Level				
WIS Station ID	WIS H_s (m)	Modeled H_s (m)	Difference (m)	Error (%)
63079	9.9	10.3	0.4	4
63095	11.0	11.7	0.7	6
63098	10.1	10.2	0.1	1
63101	10.8	11.5	0.7	6

It was also important to investigate if the 100-year synthetic storm produced the 100-year wind speed to justify a separate wind speed being used for the wind damage. This is shown in Table 1.9, which shows the synthetic 100-year storm characteristics compared to published values for storm surge, wave height, and wind speed. The storm surge values comes from NOAA, the wave height is from a WIS station, and the wind speed is from the ATC website. The table reinforces the fact that the synthetic 100-year

storm does not result in the 100-year wind speed, but again it does results in the 100-year storm surge and 100-year wave height.

Table 1.9. Comparison of the synthetic 100-year storm with published 100-year storm surge, wave height, and wind values.

100-year Storm Characteristics		
Event	NACCS 492	Published
100-year Storm Surge (m)	3.3	3.4
100-year Wave Height (m)	10.3	9.9
100-year Wind Speed (m/s)	28.3	50.0

1.3 Results

The integrated modeling system was used to perform a risk assessment to Charlestown for two main storm scenarios: Hurricane Sandy and the synthetic 100-year storm. In both scenarios simulations were performed for the dunes remaining intact as well as the dunes being eroded. Originally, a decoupled wind risk assessment was done for the 100-year wind event, and later these damage estimates were coupled with the 100-year storm surge damage estimates. The final results are presented in the form of damage maps that visually display the estimates of damage for each individual structure. For space purposes only the max structural damage is presented, but the minimum and most likely damage estimates are also readily available.

1.3.1 Historical Storm Damage Assessment

Hurricane Sandy

The first storm scenario implemented was Hurricane Sandy with the dunes remaining intact. Figure 1.27 displays the results from the SWAN+ADCIRC simulation focused on the study area, where (a) shows the water level, (b) shows the controlling wave crest height, and (c) shows the total water level. The total water level was defined as the addition of (a) the water level and (b) the controlling wave crest. It is important to note that these results showed little to no dune over-topping as a result of the dunes not being eroded. These results can be directly compared to the next simulation, which was the

scenario where the dune system was eroded, shown in Figure 1.28. The effect from removing the dunes is evident due to the increased water level and wave heights in the coastal pond. With the dunes eroded larger wave heights were capable of propagating further inland. This will result in increased damage to structures along the pond. To allow this to be more easily observed, the difference in water level, wave crest heights, and total water level between the dune eroded and dune intact cases is shown in Figure 1.29. This figure shows the removal of the dune system has a greater affect on the wave heights.

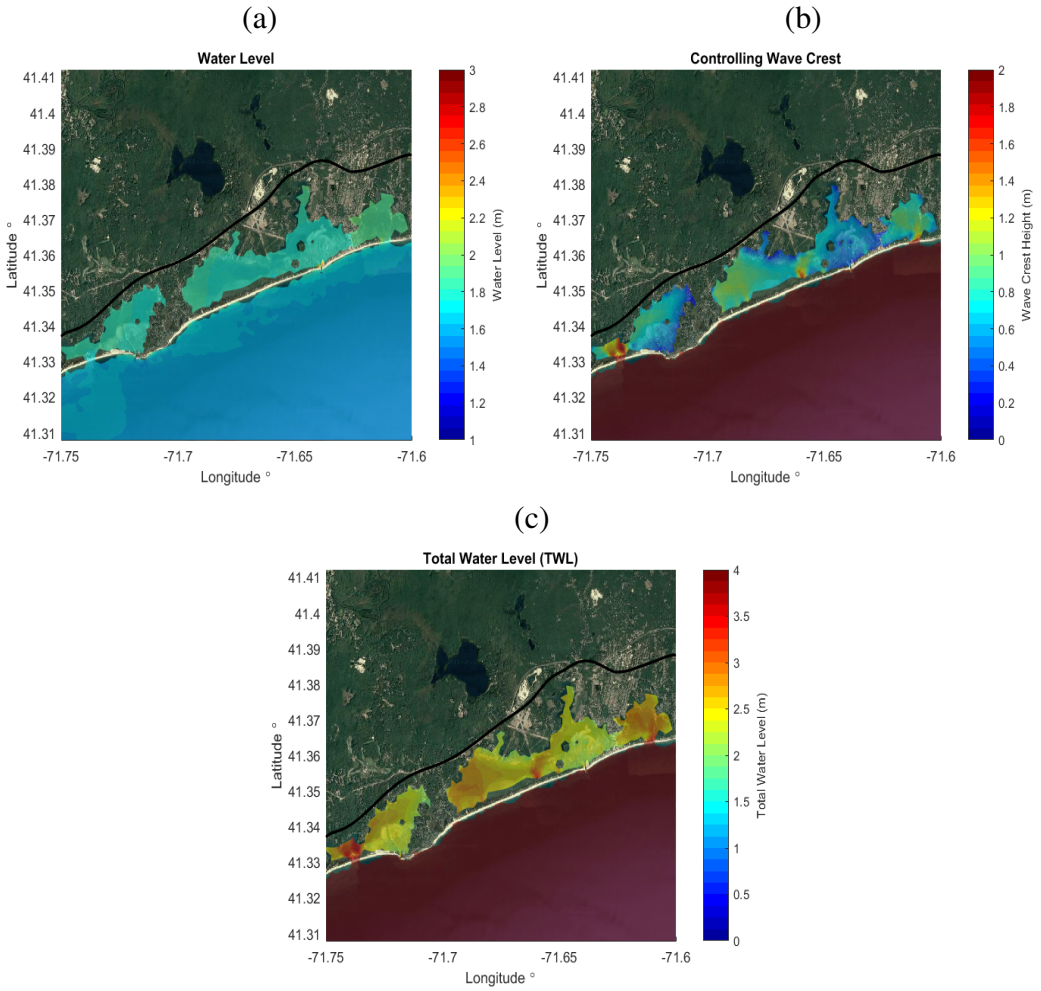

Fig. 1.27. Coupled SWAN+ADCIRC model simulation results for Hurricane Sandy with dunes intact focused on the Charlestown study area: (a) water level, (b) controlling wave crest, and (c) total water level. The black line displays the boundary of the regional model's domain, and is shown on all subsequent figures.

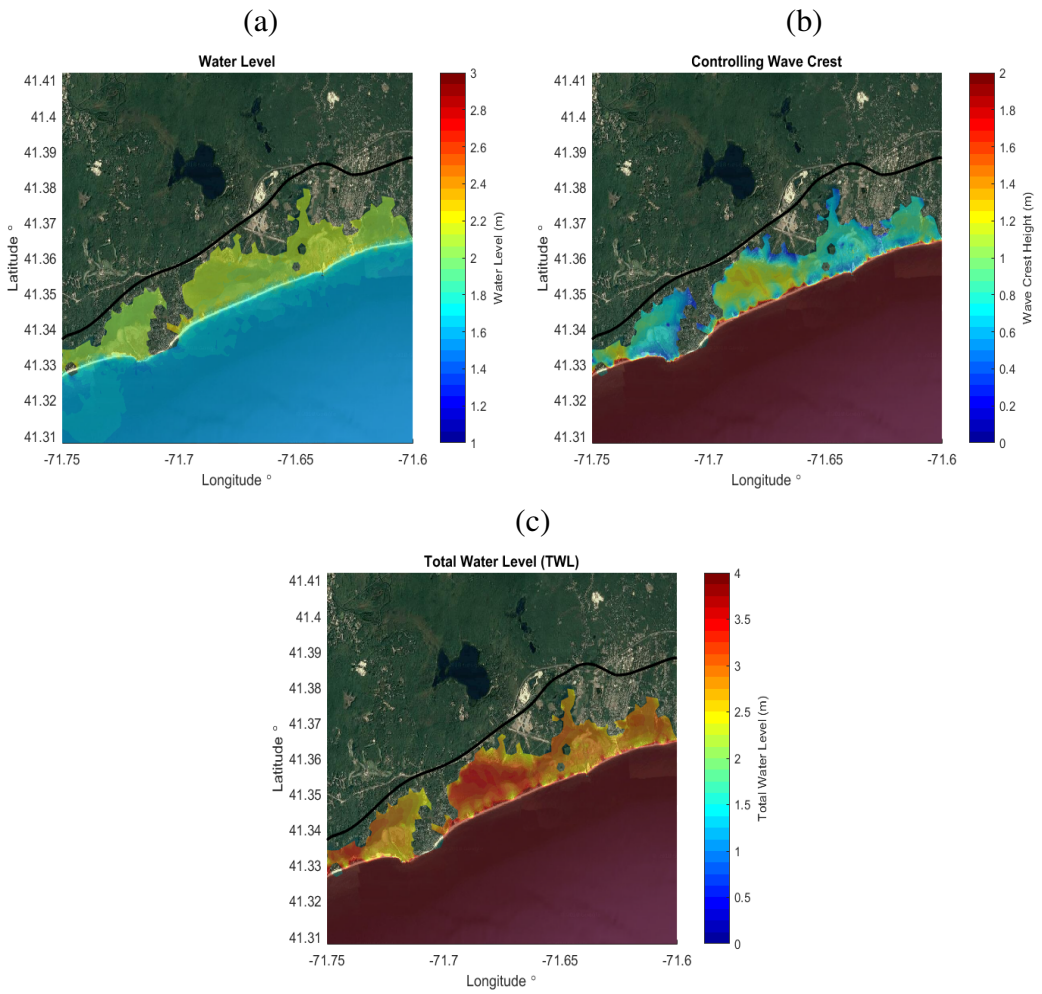

Fig. 1.28. Coupled SWAN+ADCIRC model simulation results for Hurricane Sandy with dunes eroded focused on the Charlestown study area: (a) water level, (b) controlling wave crest, and (c) total water level.

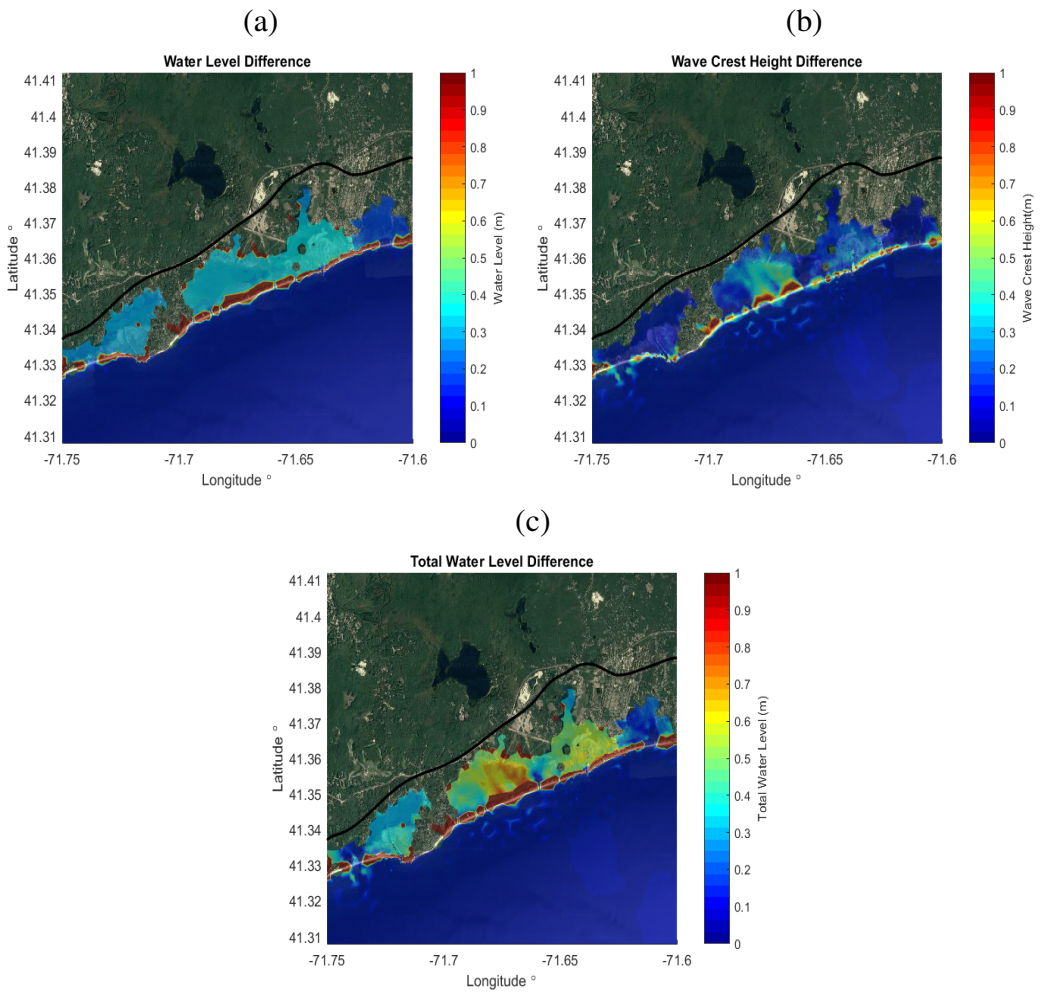

Fig. 1.29. Difference between the Hurricane Sandy results for the dunes eroded and intact: (a) water level, (b) controlling wave crest, and (c) total water level.

To further elaborate on the implications of the dune system failing, Figure 1.30 was created. This figure displays a transect taken along the dunes in front of the coastal pond, showing the total water level over the DEM for the dunes remaining intact and the dunes being eroded. As reference, this transect was taken in approximately the same location as transect 2 from the STWAVE and SWAN comparison transects. The transect in the figure aids in visualizing the effect the dunes had on the storm effects. It shows in the intact case a dune elevation that is high enough to prevent over-topping from the storm effects (red/black lines). When the transect is viewed in the eroded case the decrease in dune elevation is easily observed (roughly 2 m), leading to the uninterrupted propagation

of the storm effects into the coastal pond (blue/green lines).

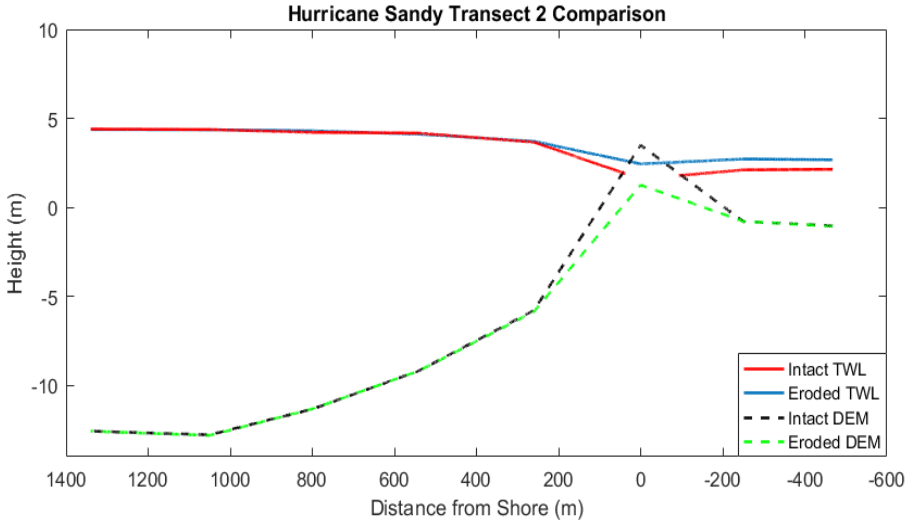

Fig. 1.30. Total water level transect taken in the Charlestown study area for Hurricane Sandy. Approximate transect location corresponds to Transect 2 shown in Figure 1.8.

The first damage estimate map is shown in Figure 1.31, corresponding to the dune intact scenario for Hurricane Sandy. The map shows that the study area was fairly resilient to the effects of Hurricane Sandy when the dunes remained intact. A total of 55 structures were estimated to experience damage, and in most cases the damage was less than 50%. Only 9 structures were estimated to have damage greater than 50%. This 50% mark was determined to be an important factor because if a structure experiences structural damage equal to or exceeding 50% the Coastal Resources Management Council (CRMC) for Rhode Island enforces the homeowner to rebuild the structure to the new building codes. The figure also shows that most of the damage that occurred in the study area was to the structures located in the low-lying areas along the coastal pond. The breakdown of damage by prototype is shown in Table 1.10.

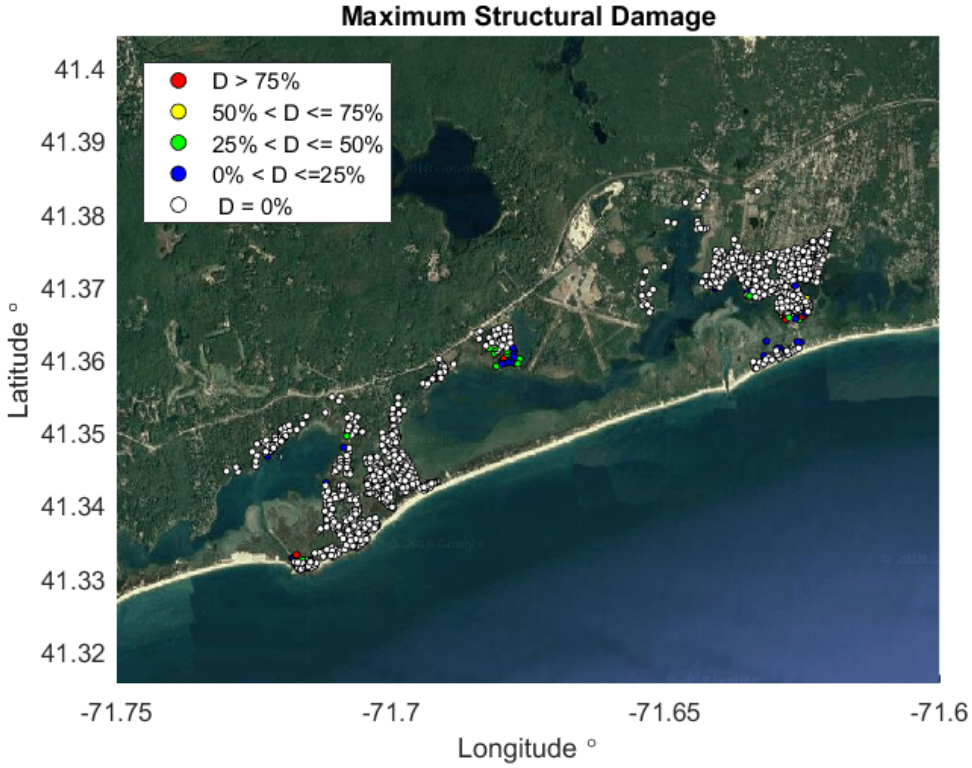

Fig. 1.31. Maximum percent damage by structure for Charlestown from Hurricane Sandy with dunes intact.

Figure 1.32 displays the damage estimate to the study area from Hurricane Sandy in the scenario where the dunes were eroded. In this case, the number of affected structures has increased, as well as the severity of damage. The total structures damaged was 160, meaning that 105 additional structures were affected due to the removal of the dunes. Additionally, 67 structures were damaged 50% or greater, which was an increase of 58 structures. This was expected as the removal of the dune system was shown to have a substantial impact on the storm effects in the study area. Table 1.10 shows the breakdown of damage by prototype, and the comparison of the estimated damage between the two scenarios for Hurricane Sandy. Unfortunately, an observed damage dataset following Hurricane Sandy was not available for comparison. This would have allowed for the validation of the modeled damage estimates. Without the model validated, the results

should not be viewed as exact damage calculations, but instead as an indicator of the high vulnerability areas in the community.

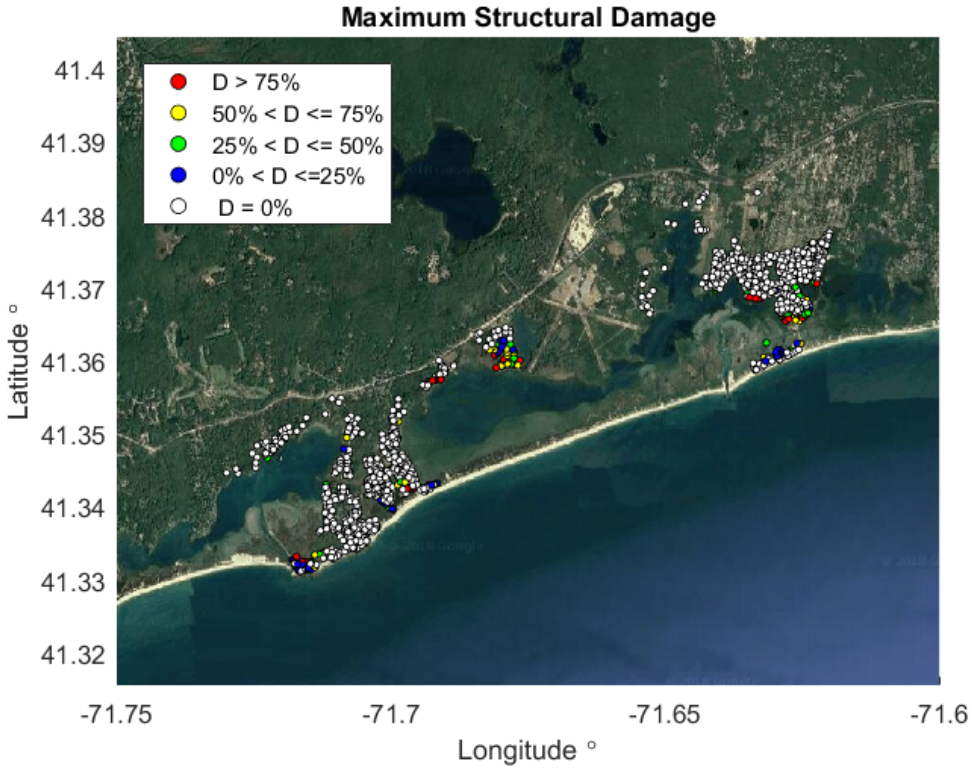

Fig. 1.32. Maximum percent damage by structure for Charlestown from Hurricane Sandy with dunes eroded.

Table 1.10. Summary of modeled structural damage for Hurricane Sandy for both dunes intact and eroded.

Dunes Intact			
Prototype	Description	Structures Damaged	Structures Damaged > 50%
5A	1 -story, no basement	4	3
6B	2-story, basement	45	6
7A	Open Stilts	2	0
7B	Enclosed Stilts	4	0
	Total Structures	**55**	**9**
Dunes Eroded			
Prototype	Description	Structures Damaged	Structures Damaged > 50%
5A	1-story, no basement	19	10
6B	2-story, basement	114	56
7A	Open Stilts	14	0
7B	Enclosed Stilts	13	1
	Total Structures	**160**	**67**

1.3.2 Future Storm Damage Assessment

Synthetic 100-year Storm Surge Event

A synthetic 100-year storm surge event from the NACCS dataset was implemented to represent a future storm for the study area. The synthetic 100-year storm was simulated for the dunes remaining intact and being eroded. The results from the coupled SWAN+ADCIRC are shown in Figure 1.33, where (a) is the water level, (b) is the controlling wave crest height, and (c) is the total water level. In the figure it can be observed that the dune system has been over-topped in several locations even with the dunes intact. Figure 1.34 displays the results for the simulation when the dune system was eroded. The main difference in these results is the entire dune area is fully over-topped with the dune system eroded. In general, the severity and flood extent remained the same in both cases. This was a result of the dune intact case also having over-topping, allowing the storm effects to propagate into the study area. The differences between the dune intact and dune eroded results are shown in Figure 1.35. This figure helps to reaffirm the conclusion that the main area of difference is along the dune system.

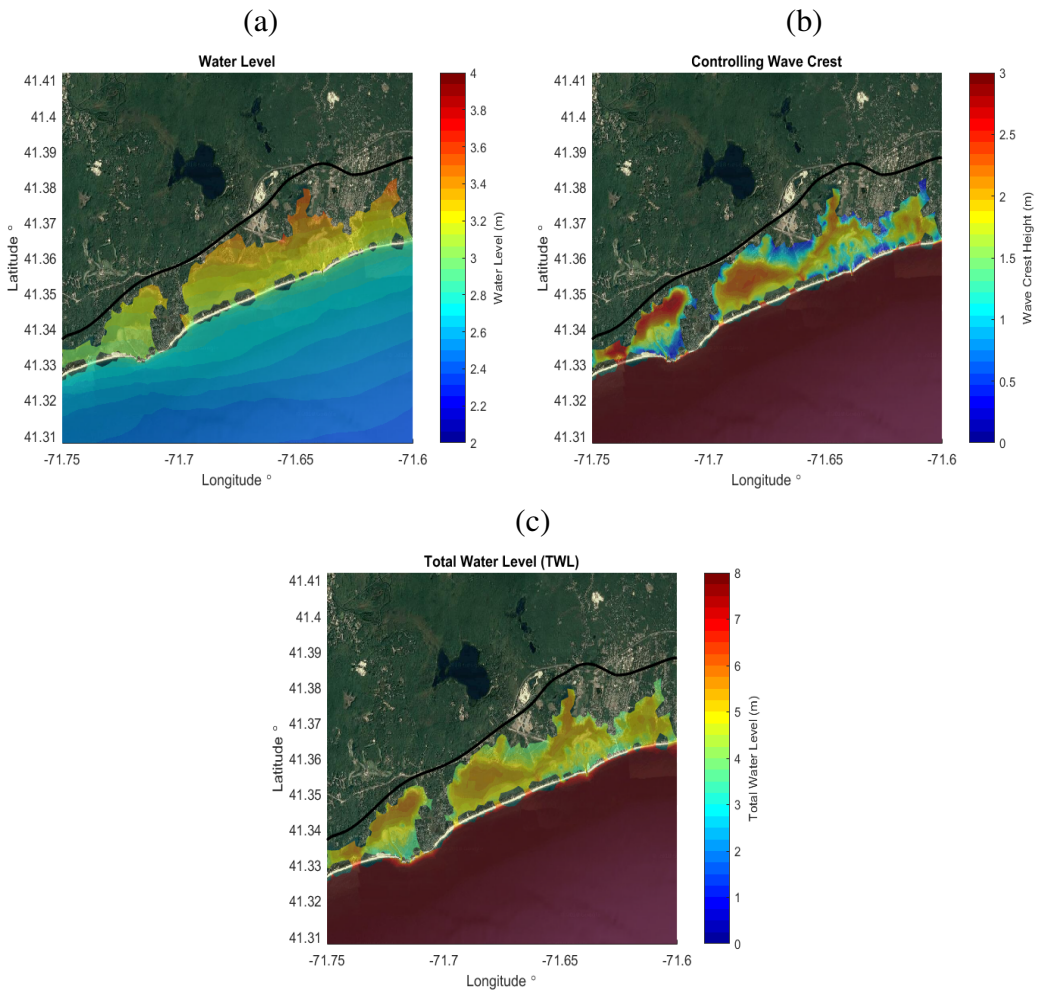

Fig. 1.33. Coupled SWAN+ADCIRC model simulation results for the synthetic 100-year storm with dunes intact focused on the Charlestown study area: (a) water level, (b) controlling wave crest, and (c) total water level.

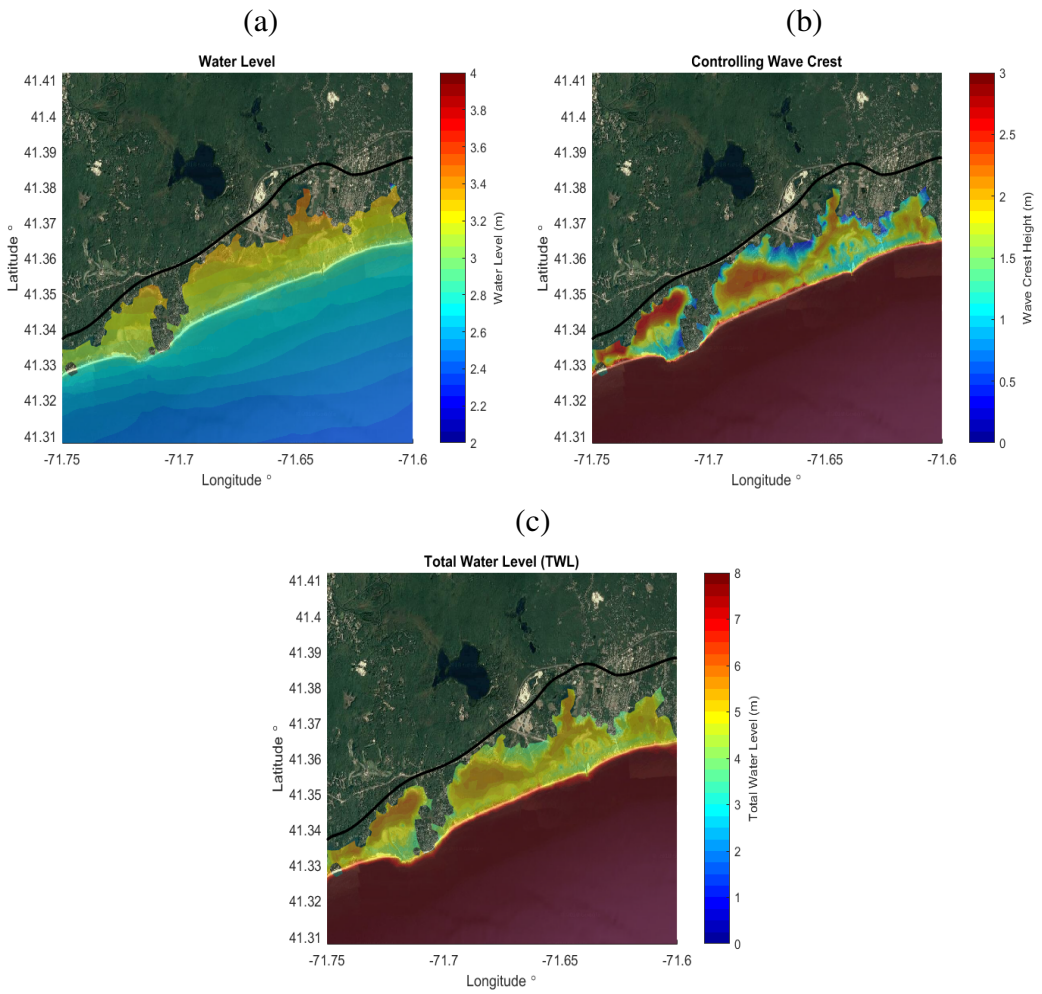

Fig. 1.34. Coupled SWAN+ADCIRC model simulation results for the synthetic 100-year storm with dunes eroded focused on the Charlestown study area: (a) water level, (b) controlling wave crest, and (c) total water level.

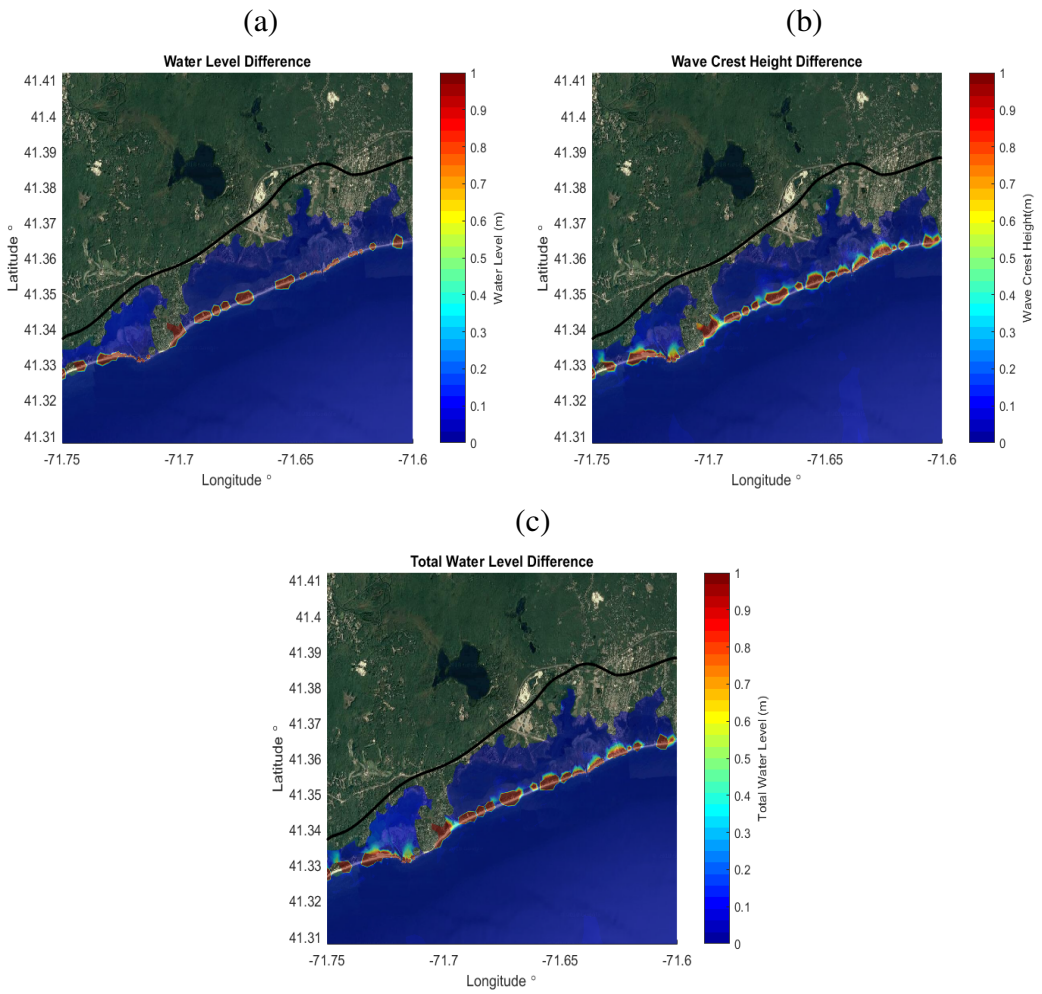

Fig. 1.35. Difference between the snythetic 100-year results for the dunes eroded and intact: (a) water level, (b) controlling wave crest, and (c) total water level.

A transect was taken in the study area to show the difference between the case of the dunes remaining intact and being eroded. The transect is shown in Figure 1.36. The dune intact DEM is shown by the black dotted line and the dune eroded DEM is shown by the green dotted line. The figure shows there was a decrease of about 2 m in the dune elevation. This transect also displays a location where the dune was able to prevent over-topping when intact (red line), but is then easily over-topped when the dunes are eroded (blue line).

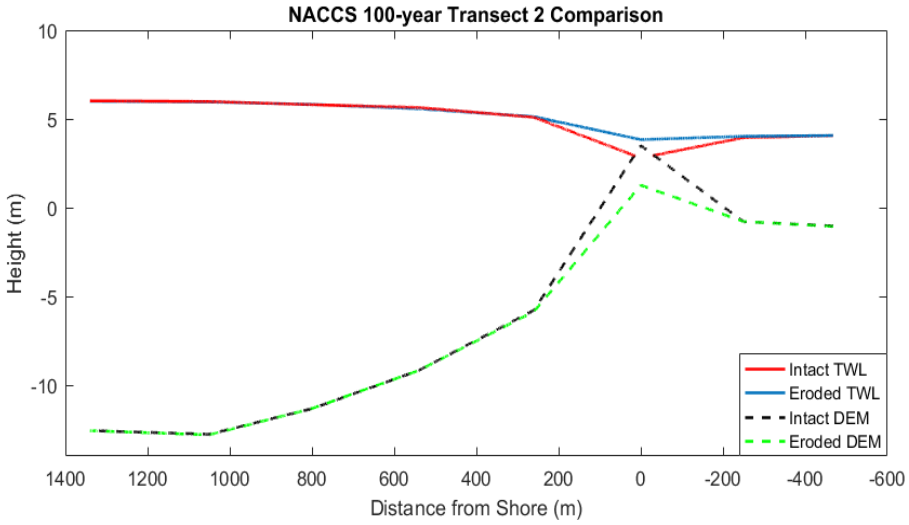

Fig. 1.36. Total water level transect taken in the Charlestown study area for the synthetic 100-year storm. Approximate transect location corresponds to Transect 2 shown in Figure 1.8.

The damage estimate for the synthetic 100-year storm with the dunes remaining intact is shown in Figure 1.37. In this case a total of 365 structures experience damage, with 316 of those structures experiencing damage 50% or greater. The damage occurred mainly to the structures in the low-lying areas surrounding the coastal pond, along with several structures near the coastline. These results show the structures that were affected by the storm were substantially impacted, with the majority being severely damaged (> 50%). The breakdown of the damage in the study area on a prototype basis is shown in Table 1.11.

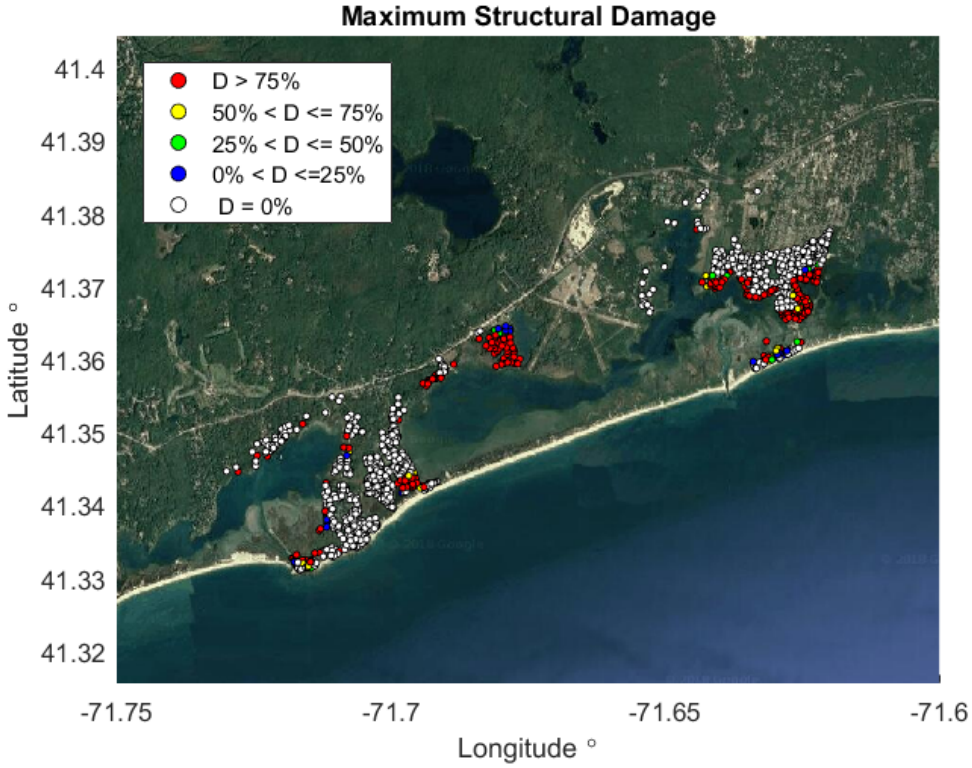

Fig. 1.37. Maximum percent damage by structure for Charlestown from the synthetic 100-year storm with dunes intact.

Figure 1.38 shows the damage estimate corresponding to the synthetic 100-year storm with the dune system eroded for the simulation. This scenario estimated a total of 414 structures being damaged, and 378 of those structures damaged 50% or greater. The very susceptible low-lying areas along the coastal pond experienced the most structural damage. This map shows an increase in the number of damaged structures along the coastline as well, which was a result of removing the dunes. The summary of damage by prototype is shown in Table 1.11. An important conclusion is that between both storm damage estimates (Hurricane Sandy and 100-year) the most affected structure was always 6B (2-story, basement). This structure type is most affected due to the presence of a basement, allowing the damage to begin occurring before storm effects reach the FFE. The same conclusion was made in other risk assessment studies for coastal areas

(Small et al., 2016; Spaulding et al., 2016).

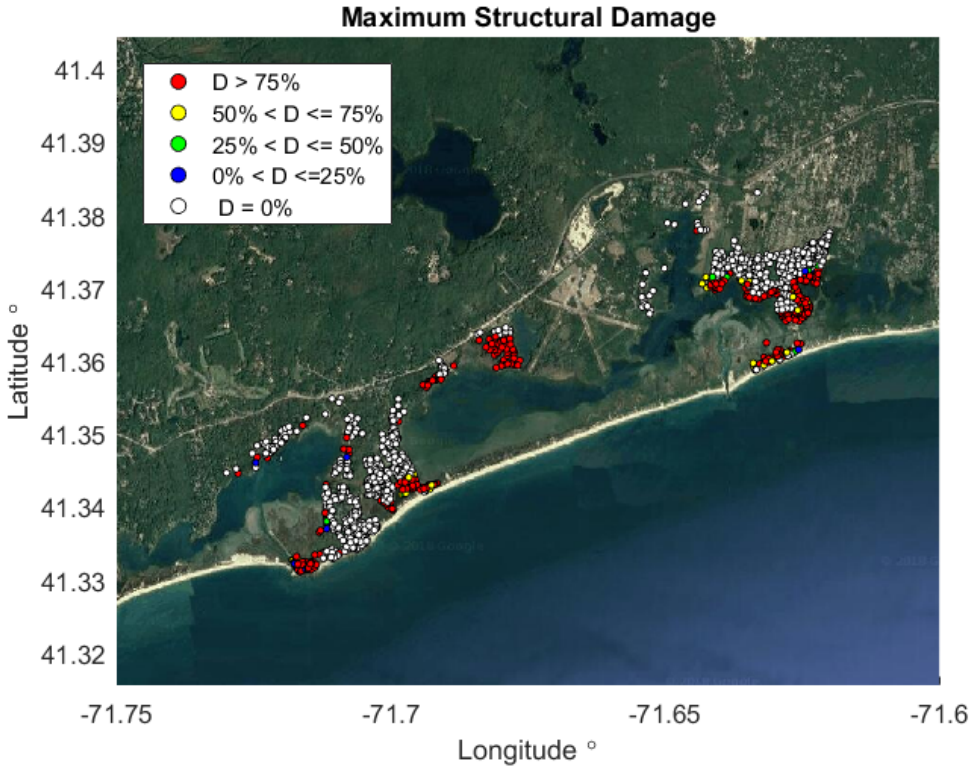

Fig. 1.38. Maximum percent damage by structure for Charlestown from the synthetic 100-year storm with dunes eroded.

Table 1.11. Summary of modeled structural damage for the synthetic 100-year storm for both dunes intact and eroded.

Dunes Intact			
Prototype	Description	Structures Damaged	Structures Damaged > 50%
5A	1-story, no basement	80	78
6B	2-story, basement	246	217
7A	Open Stilts	18	6
7B	Enclosed Stilts	21	15
	Total Structures	**365**	**316**
Dunes Eroded			
Prototype	Description	Structures Damaged	Structures Damaged > 50%
5A	1-story, no basement	85	81
6B	2-story, basement	267	242
7A	Open Stilts	29	24
7B	Enclosed Stilts	33	31
	Total Structures	**414**	**378**

A unique aspect of this study was the ability to compare this coastal risk model's results directly to another study that performed a similar risk assessment in the same study area. Spaudling et al., (2016) performed a risk assessment to Charlestown for a 100-year storm with both an intact and an eroded dune profile, and also incorporated the effects of SLR. The study implemented water levels based on NACCS save point data, and simulated waves using STWAVE with a grid resolution of 10 m (Spaulding et al., 2016). Besides the real-time forecasting option, the main differences between the two risk assessments were the numerical models and the resolution of the model domains. Both studies implement the NACCS damage functions allowing for the comparison of damage estimates.

Figure 1.39 shows the total water level comparison at the same scale between the two studies, with the major areas of difference highlighted by the purple boxes. In both the dune intact and dune eroded scenario Spaulding et al., (2016) estimates a larger flood extent and higher total water levels. The biggest difference is in the intact case for Spaulding et al., (2016) the dunes are fully over-topped. Figure 1.40 shows the damage maps for the two studies, where (a) and (b) are the comparison between the dunes intact estimates and (c) and (d) are the comparison between the dunes eroded estimates. The purple boxes indicate the major areas of difference in the number of affected structures between the two studies. The detailed comparison for each dune scenario is shown in Table 1.12 and Table 1.13, respectively. In both dune scenarios, Spaulding et al., (2016) predicts a larger number of structures to be damaged. For the dune intact case the difference in affected structures was 504, and for the dune eroded case the difference was 551 structures. The difference in the number of structures damaged greater than 50% was less dramatic, this study predicted 95 more structures in the intact scenario, and Spaulding et al., (2016) predicted 163 more structures in the dune eroded scenario. The reasons for these differences will be addressed in the discussion section.

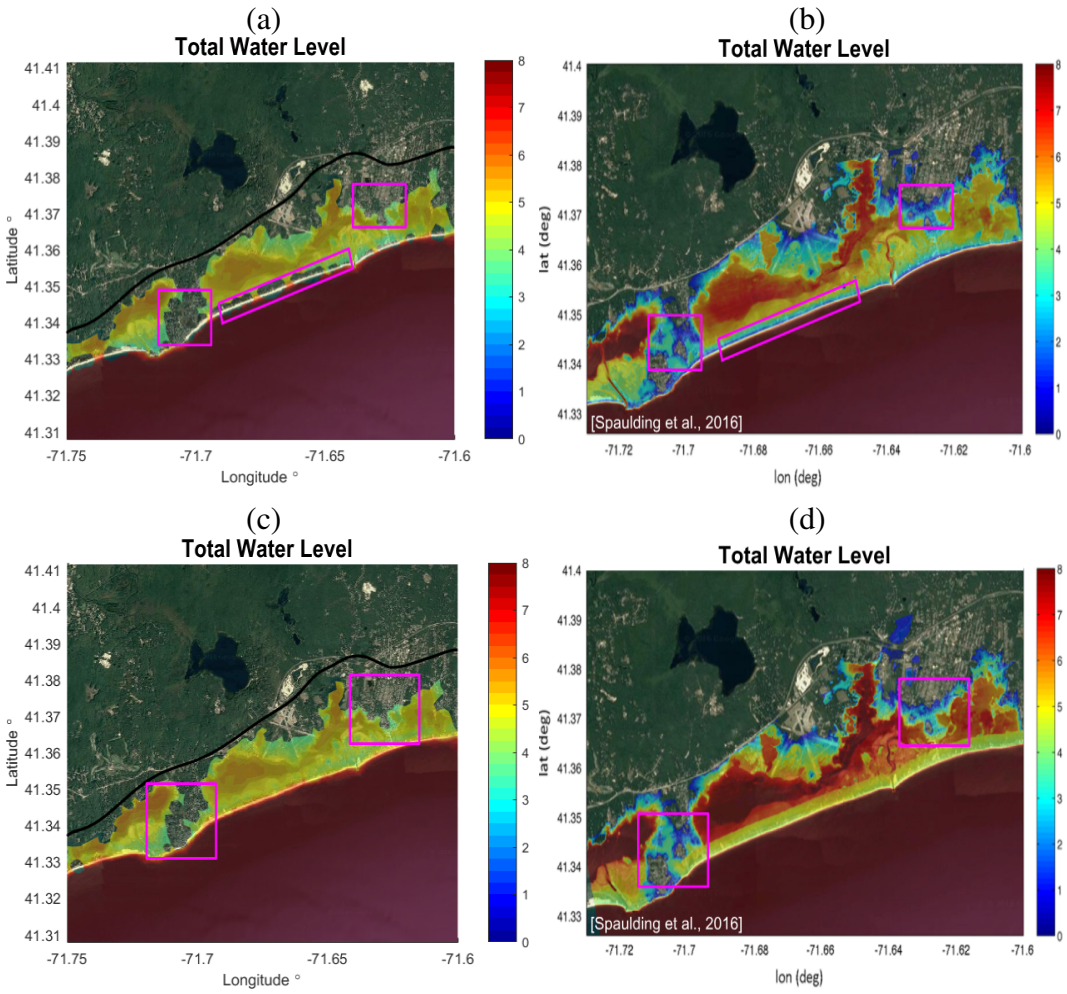

Fig. 1.39. Comparison of total water level estimates in meters with dunes intact from (a) this study and (b) Spaulding et al., (2016), and with dunes eroded from (c) this study and (d) Spaulding et al., (2016). The purple boxes denote the areas of the major differences.

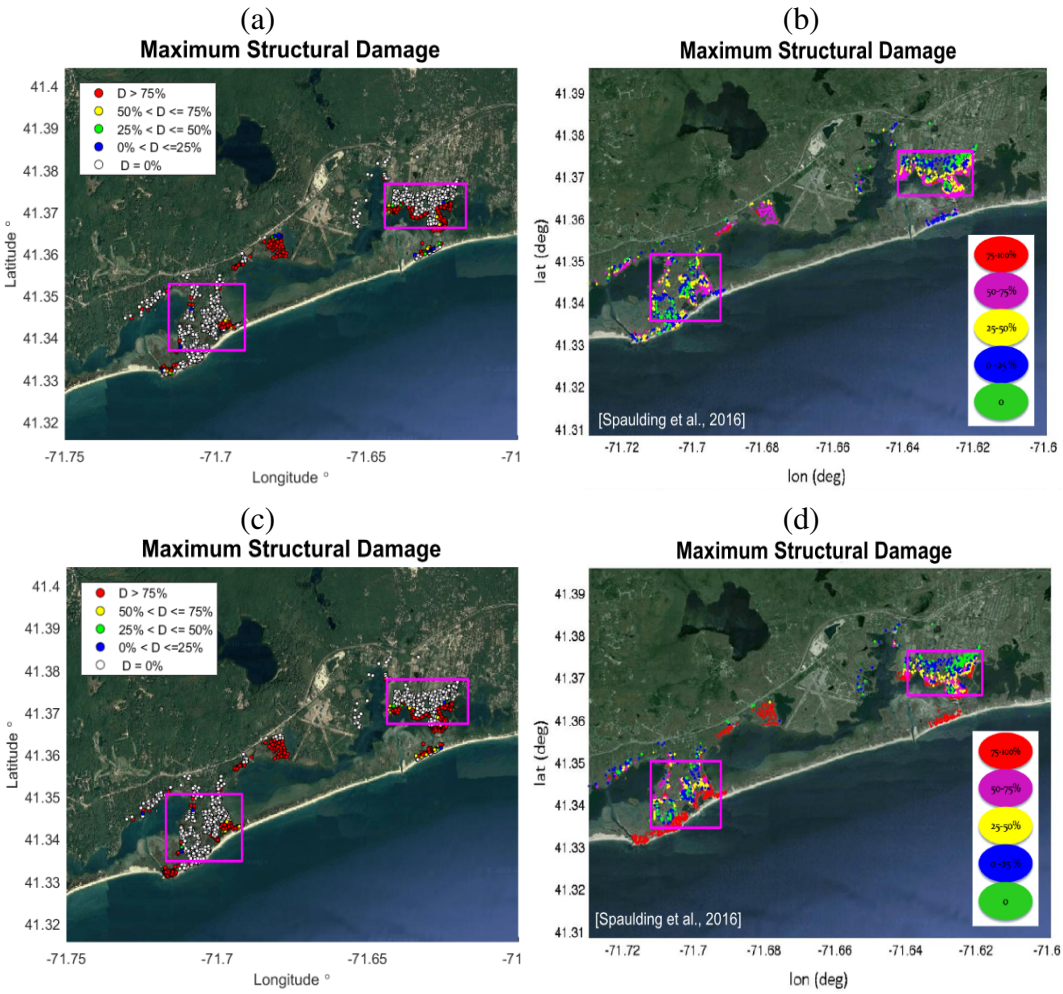

Fig. 1.40. Comparison of damage estimates with dunes intact from (a) this study and (b) Spaulding et al., (2016), and with dunes eroded from (c) this study and (d) Spaulding et al., (2016). The purple boxes denote the areas of the major differences.

Table 1.12. Comparison of modeled damage estimates between this study and Spaulding et al., (2016) for the 100-year storm with the dunes intact in Charlestown, RI. Positive difference means this study estimated more structures, and negative difference indicates the other study estimated more structures.

Dunes Intact, this Study			
Prototype	Description	Structures Damaged	Structures Damaged > 50%
5A	1-story, no basement	80	78
6B	2-story, basement	246	217
7A	Open Stilts	18	6
7B	Enclosed Stilts	21	15
	Total Structures	**365**	**316**
Dunes Intact, Spaulding et al., (2016)			
Prototype	Description	Structures Damaged	Structures Damaged > 50%
5A	1-story, no basement	189	17
6B	2-story, basement	618	204
7A	Open Stilts	27	0
7B	Enclosed Stilts	35	0
	Total Structures	**869**	**221**
Difference			
Prototype	Description	Structures Damaged	Structures Damaged > 50%
5A	1-story, no basement	-109	+61
6B	2-story, basement	-372	+13
7A	Open Stilts	-9	+6
7B	Enclosed Stilts	-14	+15
	Total Structures	**-504**	**+95**

Table 1.13. Comparison of modeled damage estimates between this study and Spaulding et al., (2016) for the 100-year storm with the dunes eroded in Charlestown, RI. Positive difference means this study estimated more structures, and negative difference indicates the other study estimated more structures.

Dunes Eroded, this Study			
Prototype	Description	Structures Damaged	Structures Damaged > 50%
5A	1-story, no basement	85	81
6B	2-story, basement	267	242
7A	Open Stilts	29	24
7B	Enclosed Stilts	33	31
	Total Structures	**414**	**378**
Dunes Eroded, Spaulding et al., (2016)			
Prototype	Description	Structures Damaged	Structures Damaged > 50%
5A	1-story, no basement	207	83
6B	2-story, basement	682	382
7A	Open Stilts	36	36
7B	Enclosed Stilts	40	40
	Total Structures	**965**	**541**
Difference			
Prototype	Description	Structures Damaged	Structures Damaged > 50%
5A	1-story, no basement	-122	-2
6B	2-story, basement	-415	-140
7A	Open Stilts	-7	-12
7B	Enclosed Stilts	-7	-9
	Total Structures	**-551**	**-163**

1.3.3 Wind Damage Assessment

100-year Wind Event

A simplistic mono-culture decoupled wind damage assessment was performed for the study area. The structures were assumed to possess the structural characteristics that would result in the most damage from wind forcing. The damage estimate for the 100-year return period wind speed (112 mph) can be viewed in Figure 1.41. This map shows that every structure in the study area experienced minimal to moderate damage. A total of 744 structures were estimated to receive damage between 1-10%, and the remaining 579 structures were estimated to be 20-30% damaged. The reason for the variation of the wind damage estimates was the surface roughness value for each structure. The lower

the surface roughness value, the more damage the structure received.

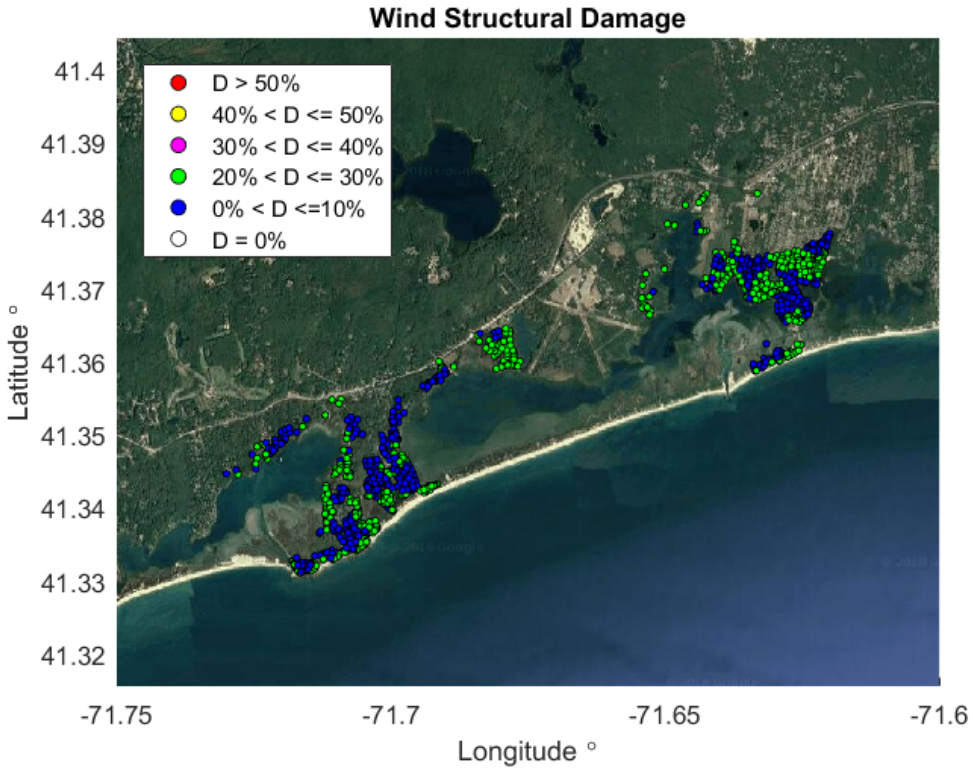

Fig. 1.41. Percent damage by structure for Charlestown from the 100-year return wind speed.

Combined Surge, Wave, and Wind Damage

Although the 100-year storm surge and 100-year wind speed are decoupled a combined damage estimate was performed as a worst case scenario for Charlestown. This estimate selected the highest value between inundation, wave, and wind damage as the damage percentage for the structure. Figure 1.42 displays the damage estimate for the synthetic 100-year storm with the dunes eroded and the 100-year wind speed of 112 mph. The results show that the severe damage was a result of the combined storm effects of inundation and waves, and the lower damage spread throughout the study area was a result of wind. In this scenario, every structure in the study area was estimated to receive damage.

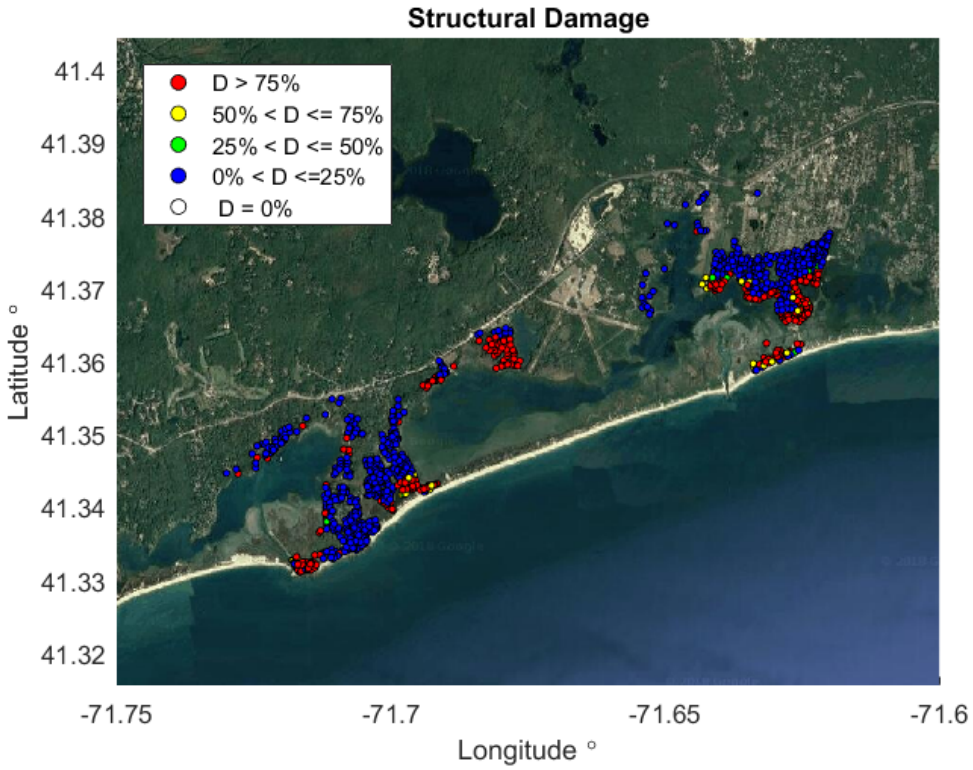

Fig. 1.42. Percent damage by structure for Charlestown from the synthetic 100-year storm surge event with dunes removed and the 100-year return wind speed.

1.4 Discussion

The coastal risk assessment in this study was performed in three phases. The first phase was the development of the integrated model system, which involved testing and validating the coupled SWAN+ADCIRC model for its ability to properly hindcast/forecast storms. This hindcast mode was tested for Hurricane Sandy using the NECOFS WRF wind data, and the results showed good agreement between the model's predictions and the recorded NOAA data for the storm. The forecast mode was verified for two large Nor'easters that occurred, one in March 2017 and one in March 2018. The model performed well when compared to the NOAA recorded data, but more discrepancies were present in these predictions. This was an expected result as the system performed forecast simulations based on forecast wind data, which has less accuracy compared to

hindcast wind data. After the coupled model was verified, the results were implemented into the coastal risk tool that was developed for this study to predict damage.

The second phase was to apply the developed model system to Charlestown, RI to predict damage for a selected historical storm. The historical storm of interest was selected to be Hurricane Sandy. When this storm impacted Rhode Island it was not as devastating as other historical storms for the study area, but resulted in some dune erosion and over-topping leading to levels of structural damage. The storm surge and wave height results from the validated model for Hurricane Sandy were fed into the risk assessment system to produce damage estimate maps on an individual structure basis. These maps were created for a dune intact scenario as well as a dune eroded scenario. During Hurricane Sandy, the dunes in the study area were not severely eroded, but the eroded scenario was performed to investigate the impact an intact dune system can have on preventing damage in smaller storm events. As expected, the number of structures affected and the severity of damage increased in the dune removed scenario. This was a result of larger wave heights propagating over the eroded dunes deeper into the study area. In the dune intact case, 55 structures experienced damage, while 160 experienced damage with the dunes removed. With the dunes intact 16% of the affected structures were damaged greater than 50%, requiring them to build to new building codes. This increased to 42% of the affected structures in the dune eroded case, indicating the protection the dune system provided. The actual damage level in the study area resulting from Hurricane Sandy was more similar to the dune intact estimates since the damage was relatively low from this storm.

Unfortunately, a drawback of this study was the lack of an observed damage report for Charlestown following the damage produced by Hurricane Sandy. Several attempts were made to obtain such a dataset, with a rapid damage assessment dataset being obtained, but this report was focused on Westerly, RI. With the lack of observed data the

damage estimates were not validated, however the results still provide valuable insight into the areas and structure types in the coastal community that were most vulnerable to storm effects. In the case of Hurricane Sandy, the most vulnerable areas were the low-lying areas directly on the coast and located around the coastal pond. The most damaged structures were those with basements as the damage begins as water enters the basement. Structures with low FFE values were also heavily damage, as the damage calculations are strongly controlled by this variable. This result is in agreement with other published risk assessment research (Small et al., 2016; Spaulding et al., 2016; Grilli et al., 2017).

The third and final phase was to demonstrate the ability of this integrated model system to be applied in forecasting mode for a tropical/extratropical storm. Since the forecast storms did not result in damage to the study area, the actual validated forecast system results were not implemented into the damage assessment. Instead a hypothetical future storm was used, which corresponded to NACCS synthetic storm #492. This storm closely matched the upper 95% 100-year storm surge value for Newport, RI, and was implemented as such a storm into the modeling system. Simulations for this synthetic storm were carried out using the coupled SWAN+ADCIRC model for both a dune intact and dune eroded scenario. Due to the magnitude of this storm the damage estimates for the dune intact scenario show substantial damage, with 365 structures damaged and 86% of those structures were damaged greater than the 50% mark. The removal of the dunes resulted in a total of 414 structures damaged, with 91% of those structures damaged greater than 50%. The damage that occurred was focused around the low-lying areas directly along the coastal ponds, as well as the lower elevated areas of the coastline. These damage estimates also show that due to the severity of the storm the majority of the structures that encountered the storm effects received critical damage (>50%). In this case, the most damaged structures were again those with basements and low FFE values.

A comparison between this study and the one performed by Spaulding et al., (2016) was made. Both risk assessments utilized a 100-year storm surge event impacting Charlestown, with Spaulding et al., (2016) implementing STWAVE as its wave model at a higher resolution than the regional domain used in this study. The comparison showed a large difference in the predicted total number of structures damaged for both the dune intact and eroded scenarios. Several factors contributed to the differences, namely boundary conditions, domain resolutions, and variations between STWAVE and SWAN. The boundary condition for surge level in Spaulding et al., (2016) was derived from the NACCS upper 95% confidence interval for the 100-year surge at NACCS save points (Spaulding et al., 2015). At Newport this value is 3.93 m, which is 0.66 m higher than the surge at Newport caused by the synthetic 100-year storm implemented in this study. This increased water level would result in a larger flood extent, and allow larger wave heights in the study area, increasing the total structures impacted. The resolution of the domains were different in the study area, with the STWAVE resolution being much higher (10 m) compared to the SWAN+ADCIRC varying resolution (10 m to 100 m). This difference in resolution could lead to SWAN+ADCIRC underestimating the flood extent, which would decrease the number of affected structures. The final reason for the differences was attributed to the variations between STWAVE and SWAN that were investigated in the methods section. As that section showed, it is possible that STWAVE estimated wave heights on the order of 1 m or so higher than SWAN. This wave height difference would be amplified by the increased surge level between the simulations as well, resulting in more structures being damaged. The SWAN wave height calculations were also done on a time-varying solution. It is not possible to determine the more accurate risk assessment model, as neither have been validated, but both are useful tools in highlighting the high risk areas in coastal communities. Both models highlighted the vulnerability of the structures located around the coastal pond, and the structures located

on the lower-lying areas of the dune system.

This risk assessment system also implemented simplified wind damage estimates using Hazus fragility curves. The 100-year wind speed used for this assessment was 112 mph, which resulted in damage to every structure in the study area ranging from 1-30%. Although the damage estimates were wide-spread the severity of the damage from the 100-year wind alone, even for the most susceptible structure characteristics, was fairly low compared to the 100-year storm surge damage. This result leads to the conclusion that in a large storm event (100-year storm surge or wind) the immediate effects of storm surge and wave heights will be more damaging, but the wind damage will be much more widespread. The possible combination of the effects can be devastating to coastal communities.

A worst-case scenario was implemented in the risk assessment. This corresponded to a 100-year storm surge and 100-year wind event occurring simultaneously with the dune system eroded. In this case, the storm effects dominated the damage around the coastal pond and coastline, and the wind damage dominated the rest of the study area. The damage estimates for this scenario were clearly the worst as every structure was affected.

Several sources of uncertainty can lead to inaccuracy in the presented results. Figure 1.43 shows the flowchart of the system color-coded according to the level of uncertainty for each section. The higher the number/the darker the gray the more uncertainty in that section. As the figure shows, the wind data, numerical models, and damage functions contain uncertainty, and therefore the damage estimates do as well. The area with the least uncertainty is the coupled SWAN+ADCIRC model because it was validated at several locations. The area with the highest uncertainty is the risk assessment model, because all of the previous levels of uncertainty propagate forward and are brought together into the risk model.

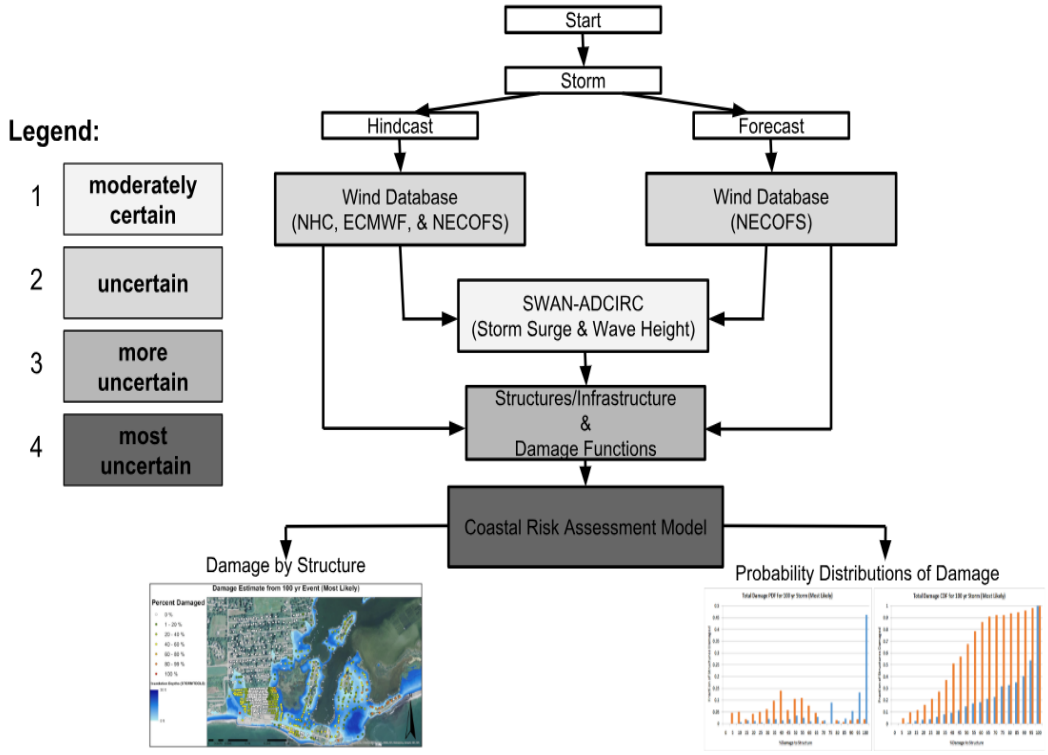

Fig. 1.43. Flowchart of the integrated modeling system with each section containing uncertainty highlighted with a corresponding ranking. The higher number/darker gray means more uncertainty is associated with that section.

The accuracy of wind data is crucial to the accurate prediction of storm surge and wave heights. Torres et al., (2017) showed that wind data with an error within 20% of the observed peak wind speed can still successfully be used to accurately model storm surge and wave heights. This study also showed implementing poor wind data can result in error as high as 50% in storm surge and wave height predictions (Torres et al., 2017). The uncertainty in the wind data increases when dealing with forecast wind products, as shown in the forecast model validations.

Numerical storm surge and wave models inherently contain a level of uncertainty, which was investigated during the validation process. However, this validation has not been performed for wave heights in the coastal zones/ponds due to the lack of observed data leading to uncertainty in this area. Even with the models validated there was still

the potential for uncertainty throughout the domain due to possible resolution issues. A study investigating the sensitivity of SWAN+ADCIRC results to domain resolution found that for open areas coarse resolution (100 m to 500 m) was acceptable, but for more inland areas (inlets, wetlands, rivers, and intertidal zones) resolution needs to be improved (Kerr et al., 2013). The study found that a resolution between 30 m and 80 m was sufficient for the inland areas, with the higher the resolution the better. The regional model's domain resolution in the study area varies from 20 m in the inlets and coastal ponds to 200 m near the coast. For this study the resolution is adequate, but to avoid possible uncertainty resulting from domain resolution future studies should increase the selected study area resolution.

The largest uncertainty was in the NACCS damage functions, which was addressed in the introduction section as well. These functions were based on observed damage data, but these recordings were performed using a best guess as to what the actual water level and corresponding wave height was at a location. Then these were attempted to be related to percent of structural damage for an individual structure. Although there might not be a better method to do this type of analysis it will lead to both over- and under-estimates in the water levels, wave heights, and structural damage at each site, leading to uncertainty in the damage estimates. In the case of Hurricane Sandy this uncertainty could have been investigated if an observed damage report for Charlestown was found to compare to the model's damage results. Unfortunately, this was not the case. Without a measure to compare the results to, the accuracy of the damage estimates cannot be determined. This risk assessment system also ignores the process of wave runup, which has the ability to increase the flood extent, and therefore the damage.

Investigating all the possible sources of uncertainty further was beyond the scope of this study. However, because of these mentioned uncertainties it is important to view the results more as a risk indicator rather than an exact structural damage calculator.

This means that if one region showed numerous structures to be severely damage during a storm, it is reasonable to assume that this area has high risk. Similar uncertainty conclusions for damage assessments on a structure-by-structure basis were made in other studies as well (Friedland, 2009; Grilli et al., 2017).

1.5 Conclusions

An integrated coastal risk assessment system was developed as a tool to forecast the threat coastal communities face from significant storm effects. This system was comprised of a coupled SWAN+ADCIRC model and a Matlab based risk assessment model. The coupled wave-surge model is capable of predicting storm surge and wave heights for both hindcast and forecast storm scenarios, and the risk model calculates damage from storm surge, waves, and wind. This is notable, as previous works have not provided an option for the real-time risk assessment of an approaching storm. In the forecast mode the coupled model was validated for two large Nor'easters that impacted the region, and performed well in both instances. The current configuration would allow the system to perform the risk assessment a full 3 days prior to the storm making an impact to the region. This system has been developed to be universally applicable to any coastal area as long as an ADCIRC domain has been developed.

The system was first implemented for Charlestown, a vulnerable coastal community in southern Rhode Island. It was tested for Hurricane Sandy and a synthetic 100-year storm that acted as a possible future storm for the study area. For each storm, simulations were performed assuming the dunes remained intact and became eroded. As the results showed, the ability to run these simulations for both dune scenarios is essential. The difference between the number of structures and severity of estimated damage was significant between the intact and eroded cases. For Hurricane Sandy, the number of impacted structures with the dunes intact was 55 and with the dunes eroded was 160, an increase of 105 structures. Of those structures affected 16% and 42% would

have to rebuild to new standards, respectively. An interesting finding was the removal of the dunes had a greater impact on the Hurricane Sandy damage results compared to the 100-year event. This was because the 100-year event over-tops the dunes in both the intact and eroded cases, resulting in less of a change in storm effects for the study area. For this event, the number of structures affected in the dune intact case was 365 and was 414 in the dune eroded case. This is an increase of 49, which was less when compared to Hurricane Sandy showing the dune system provides more protection in the smaller storm events. The 100-year event severely damaged the structures it impacted, resulting in 86% and 91% of the structures to be damage greater than 50% in the dune intact and eroded cases, respectively. This reinforces the conclusion that the dune system does not provide as much protection in the large storm events. In both storm scenarios investigated, the most vulnerable structures were two-story structures with basements, and the most resilient were elevated structures. The structures located in the low-lying areas around the coastal pond were also found to be very vulnerable in all scenarios.

A mono-culture wind damage assessment was implemented in this study as well, performed for a decoupled scenario (100-year wind only) and a worst case coupled scenario (100-year surge and 100-year wind event). The results from both cases show that the wind damage was relatively low, between 1-30%, but was widespread throughout the study area affecting all 1,323 structures. The location dependent surface roughness parameter was the crucial characteristic in determining wind damage. Both scenarios conclude that the critical damage to vulnerable coastal communities will primarily be a result of the storm surge and wave effects, as no structure was damage greater than 50% from just wind.

Regardless of the uncertainty present, this coastal risk assessment system is useful in identifying the high risk areas in vulnerable coastal communities. Once identified, the best adaptation and mitigation strategy can be determined and applied for hazard

protection. The capability of real-time forecasting of individual structure risk is unique to this system, and can provide vital information on approaching storms. With the predicted change in frequency and intensity of future storms resulting from climate change, this risk tool should prove beneficial for vulnerable coastal regions.

There are some future recommendations that would have been investigated/implemented using this system if time allowed. The first is to increase the model resolution in Charlestown (or selected study area) to fully capture the dune profile. This would allow for a more thorough analysis of the affect the erosion of the dunes has on the simulation results. Along the same line, a nearshore flood zone model could be implemented, such as Xbeach, that would be dynamically capable of simulating dune erosion instead of assuming a static profile, which is unrealistic. As mentioned earlier these types of models are very computationally expensive, and would not be practical to implement in the forecast mode of the system. The wind damage assessment could easily be improved if all the necessary structural information was known. Another worthwhile task would be attempting to determine the economic loss in terms of cost for each damage estimate. This would require parcel information that provides the structure value, and the development of a metric to convert structural damage to value loss. The final recommendation would be to leverage to system to investigate different mitigation measures, such as elevating structures and artificial dunes, and perform a cost benefit analysis on the reduction of damage compared to the necessary cost for the corresponding mitigation strategy.

List of References

Beardsley, R. and Chen, C. (2014). Northeast coastal ocean forecast system (necofs): A multi-scale global-regional-estuarine fvcom model. In *AGU Fall Meeting Abstracts*.

Bianchi, C., Folkert, L., Knight, J.-A., Madison, H., Maroukis, M., Quinn, B., Schicho, J., and White, M. (2017). Assessment of Damage for the Misquamicut, ri Community from a 100 Year Storm Event and Sea Level Rise.

Booij, N., Ris, R., and Holthuijsen, L. H. (1999). A third-generation wave model for coastal regions: 1. model description and validation. *Journal of geophysical research: Oceans*, 104(C4):7649–7666.

Chen, C., Bardsley, R., and Cowles, G. (2006). An Unstructured Grid, Finite-Volume Coastal Ocean Model (FVCOM) System. *Oceanography*, 19(1):78–79.

Dietrich, J., Zijlema, M., Westerink, J., Holthuijsen, L., Dawson, C., Luettich Jr, R., Jensen, R., Smith, J., Stelling, G., and Stone, G. (2011). Modeling hurricane waves and storm surge using integrally-coupled, scalable computations. *Coastal Engineering*, 58(1):45–65.

Dietrich, J. C., Tanaka, S., Westerink, J. J., Dawson, C., Luettich, R., Zijlema, M., Holthuijsen, L. H., Smith, J., Westerink, L., and Westerink, H. (2012). Performance of the unstructured-mesh, swan+ adcirc model in computing hurricane waves and surge. *Journal of Scientific Computing*, 52(2):468–497.

Ellingwood, B. R., Rosowsky, D. V., Li, Y., and Kim, J. H. (2004). Fragility assessment of light-frame wood construction subjected to wind and earthquake hazards. *Journal of Structural Engineering*, 130(12):1921–1930.

FEMA (2012). *Multi-hazard Loss Estimation Methodology, Hurricane Model, Hazus MH 2.1*. Department of Homeland Security, Federal Emergency Management Agency, 2.1 edition.

FEMA (2015). Coastal Mapping Basics. [Online]. Available: http://www.region2coastal.com/resources/coastal-mapping-basics/.

FEMA (2018). Coastal Numerical Models Meeting the Minumum Requirement of the National Flood Insurance Program. [Online]. Available: https://www.fema.gov/coastal-numerical-models-meeting-minimum-requirement-national-flood-insurance-program.

Fleming, J. G., Fulcher, C. W., Luettich, R. A., Estrade, B. D., Allen, G. D., and Winer, H. S. (2008). A real time storm surge forecasting system using adcirc. In *Estuarine and Coastal Modeling (2007)*, pages 893–912.

Friedland, C. (2009). *Residential building damage from hurricane storm surge: proposed methodologies to describe, assess and model building damage*. phdthesis, Louisiana State University.

Glahn, B., Taylor, A., Kurkowski, N., and Shaffer, W. A. (2009). The role of the slosh model in national weather service storm surge forecasting. *National Weather Digest*, 33(1):3–14.

Grilli, A., Spaulding, M., Damon, C., O'Rielly, C., and Potty, G. (2012). Wind resource assessment and siting of wind energy facilities in Rhode Island. techreport, University of Rhode Island.

Grilli, A., Spaulding, M. L., Oakley, B. A., and Damon, C. (2017). Mapping the coastal risk for the next century, including sea level rise and changes in the coastline: application to charlestown ri, usa. *Natural Hazards*, 88(1):389–414.

Hamid, S., Kibria, B. G., Gulati, S., Powell, M., Annane, B., Cocke, S., Pinelli, J.-P., Gurley, K., and Chen, S.-C. (2010). Predicting losses of residential structures in the state of florida by the public hurricane loss evaluation model. *Statistical methodology*, 7(5):552–573.

Hayward, S. (2017). Development of a Realtime Wave and Storm Surge Forecasting Model for Rhode Island. M. eng. thesis, University of Rhode Island.

Jonkman, S. N., Bočkarjova, M., Kok, M., and Bernardini, P. (2008). Integrated hydrodynamic and economic modelling of flood damage in the netherlands. *Ecological economics*, 66(1):77–90.

Kerr, P., Martyr, R., Donahue, A., Hope, M., Westerink, J., Luettich, R., Kennedy, A., Dietrich, J., Dawson, C., and Westerink, H. (2013). Us ioos coastal and ocean modeling testbed: Evaluation of tide, wave, and hurricane surge response sensitivities to mesh resolution and friction in the gulf of mexico. *Journal of Geophysical Research: Oceans*, 118(9):4633–4661.

Lee, K. H. and Rosowsky, D. V. (2005). Fragility assessment for roof sheathing failure in high wind regions. *Engineering Structures*, 27(6):857–868.

Li, Y. and Ellingwood, B. R. (2006). Hurricane damage to residential construction in the us: Importance of uncertainty modeling in risk assessment. *Engineering structures*, 28(7):1009–1018.

Li, Y., van de Lindt, J. W., Dao, T., Bjarnadottir, S., and Ahuja, A. (2011). Loss analysis for combined wind and surge in hurricanes. *Natural hazards review*, 13(1):1–10.

Luettich, R., Westerink, J., and Scheffner, N. (1992). ADCIRC: an Advanced Three-Dimensional Circulation Model for Shelves, Coasts, and Estuaries, Report 1: Theory and Methodology of ADCIRC-2DDI and ADCIRC03DL. Technical Report Dredging Research Program Technical Report DRP-92-6, U.S. Army Engineers Waterways Experiment Station.

Mattocks, C. and Forbes, C. (2008). A real-time, event-triggered storm surge forecasting system for the state of north carolina. *Ocean Modelling*, 25(3-4):95–119.

NHC (2018). NHC data archive. [Online]. Available: https://www.nhc.noaa.gov/data/.

NOAA (2013). Annual exceedance probability curves. [Online]. Available: https://tidesandcurrents.noaa.gov/est/curves.shtml?stnid=8452660.

NOAA (2018). Sea Level Rise Viewer.

Oakley, B. (2016). Generalized 1Quonochontaug Barriers, Rhode Island. Technical report, Rhode Island: Shoreline Change Special Area Management Plan.

Parris, A., Bromirski, P., Burkett, V., Cayan, D., Culver, M., Hall, J., Horton, R., Knuuti, K., Moss, R., Obeyeskera, J., Sallenger, A., and Weis, J. (2012). Global Sea Level Rise Scenarious for the United States National Climate Assessment. Technical report, NOAA.

Pinelli, J.-P., Pita, G., Gurley, K., Torkian, B., Hamid, S., and Subramanian, C. (2011). Damage characterization: Application to florida public hurricane loss model. *Natural Hazards Review*, 12(4):190–195.

Ris, R., Holthuijsen, L., and Booij, N. (1999). A third-generation wave model for coastal regions: 2. verification. *Journal of Geophysical Research: Oceans*, 104(C4):7667–7681.

Roelvink, D., Reniers, A., Van Dongeren, A., de Vries, J. v. T., McCall, R., and Lescinski, J. (2009). Modelling storm impacts on beaches, dunes and barrier islands. *Coastal engineering*, 56(11-12):1133–1152.

Scawthorn, C., Flores, P., Blais, N., Seligson, H., Tate, E., Chang, S., Mifflin, E., Thomas, W., Murphy, J., Jones, C., et al. (2006). Hazus-mh flood loss estimation methodology. ii. damage and loss assessment. *Natural Hazards Review*, 7(2):72–81.

Schambach, L., Grilli, A. R., Grilli, S. T., Hashemi, M. R., and King, J. W. (2018). Assessing the impact of extreme storms on barrier beaches along the atlantic coastline: Application to the southern rhode island coast. *Coastal Engineering*, 133:26–42.

Small, C., Blanpied, T., Kauffman, A., O'Neil, C., Proulx, N., Rajacich, M., Simpson, H., White, J., Spaulding, M. L., Baxter, C. D., et al. (2016). Assessment of damage and adaptation strategies for structures and infrastructure from storm surge and sea level rise for a coastal community in rhode island, united states. *Journal of Marine Science and Engineering*, 4(4):67.

Smith, J. M., Sherlock, A. R., and Resio, D. T. (2001). Stwave: Steady-state spectral wave model user's manual for stwave, version 3.0. Technical report, Engineer Research and Development Center Vicksburg, MS Coastal and Hydrualics Lab.

Spaulding, M., Grilli, A., Damon, C., Crean, T., Fugate, G., Oakley, B., and Stempel, P. (2016). STORMTOOLS: Coastal environmental risk index (CERI). *Journal of Marine Science and Engineering*, 4(3):54.

Spaulding, M., Isaji, L., Damon, C., and Fugate, G. (2015). Application of STORMTOOLS's simplified flood inundation model, with and wihtout sea level rise, to RI coastal waters. *ASCE Solutions to Coastal Disasters Conference, Boston, MA*.

Tomiczek, T., Kennedy, A., and Rogers, S. (2013). Collapse limit state fragilities of wood-framed residences from storm surge and waves during hurricane ike. *Journal of Waterway, Port, Coastal, and Ocean Engineering*, 140(1):43–55.

Torres, M., Hashemi, M. R., Hayward, S., Spaulding, M., Ginis, I., and Grilli, S. (2017). The Role of Hurricane Wind Models in the Accurate Simulation of Storm Surge and Waves. *ASCE Journal of Waterway, Port, Coastal and Ocean Engineering Online Collection*, in review.

USACE (2015). North Atlantic Coast Comprehensive Study. Resilient Adaptation to Increasing Risk. [Online]. Available: http://www.nad.usace.army.mil/Portals/40/docs/NACCS/10A_PhysicalDepthDmgFxSummary_26Jan2015.pdf.

Vickery, P. J., Skerlj, P. F., Lin, J., Twisdale Jr, L. A., Young, M. A., and Lavelle, F. M. (2006). Hazus-mh hurricane model methodology. ii: Damage and loss estimation. *Natural Hazards Review*, 7(2):94–103.

BIBLIOGRAPHY

Beardsley, R. and Chen, C., "Northeast coastal ocean forecast system (necofs): A multi-scale global-regional-estuarine fvcom model," in *AGU Fall Meeting Abstracts*, 2014.

Bianchi, C., Folkert, L., Knight, J.-A., Madison, H., Maroukis, M., Quinn, B., Schicho, J., and White, M., "Assessment of Damage for the Misquamicut, ri Community from a 100 Year Storm Event and Sea Level Rise," May 2017.

Booij, N., Ris, R., and Holthuijsen, L. H., "A third-generation wave model for coastal regions: 1. model description and validation," *Journal of geophysical research: Oceans*, vol. 104, no. C4, pp. 7649–7666, 1999.

Chen, C., Bardsley, R., and Cowles, G., "An Unstructured Grid, Finite-Volume Coastal Ocean Model (FVCOM) System," *Oceanography*, vol. 19, no. 1, pp. 78–79, Mar. 2006.

Dietrich, J. C., Tanaka, S., Westerink, J. J., Dawson, C., Luettich, R., Zijlema, M., Holthuijsen, L. H., Smith, J., Westerink, L., and Westerink, H., "Performance of the unstructured-mesh, swan+ adcirc model in computing hurricane waves and surge," *Journal of Scientific Computing*, vol. 52, no. 2, pp. 468–497, 2012.

Dietrich, J., Zijlema, M., Westerink, J., Holthuijsen, L., Dawson, C., Luettich Jr, R., Jensen, R., Smith, J., Stelling, G., and Stone, G., "Modeling hurricane waves and storm surge using integrally-coupled, scalable computations," *Coastal Engineering*, vol. 58, no. 1, pp. 45–65, 2011.

Ellingwood, B. R., Rosowsky, D. V., Li, Y., and Kim, J. H., "Fragility assessment of light-frame wood construction subjected to wind and earthquake hazards," *Journal of Structural Engineering*, vol. 130, no. 12, pp. 1921–1930, 2004.

FEMA, *Multi-hazard Loss Estimation Methodology, Hurricane Model, Hazus MH 2.1*, 2nd ed., Department of Homeland Security, Federal Emergency Management Agency, 2012.

FEMA. U.S. Department of Homeland Security. "Coastal Mapping Basics." Apr. 2015. [Online]. Available: http://www.region2coastal.com/resources/coastal-mapping-basics/

FEMA. "Coastal Numerical Models Meeting the Minumum Requirement of the National Flood Insurance Program." 2018. [Online]. Available: https://www.fema.gov/coastal-numerical-models-meeting-minimum-requirement-national-flood-insurance-program

Fleming, J. G., Fulcher, C. W., Luettich, R. A., Estrade, B. D., Allen, G. D., and Winer, H. S., "A real time storm surge forecasting system using adcirc," in *Estuarine and Coastal Modeling (2007)*, 2008, pp. 893–912.

Friedland, C., "Residential building damage from hurricane storm surge: proposed methodologies to describe, assess and model building damage," phdthesis, Louisiana State University, 2009.

Glahn, B., Taylor, A., Kurkowski, N., and Shaffer, W. A., "The role of the slosh model in national weather service storm surge forecasting," *National Weather Digest*, vol. 33, no. 1, pp. 3–14, 2009.

Grilli, A., Spaulding, M., Damon, C., O'Rielly, C., and Potty, G., "Wind resource assessment and siting of wind energy facilities in Rhode Island," University of Rhode Island," techreport, Apr. 2012.

Grilli, A., Spaulding, M. L., Oakley, B. A., and Damon, C., "Mapping the coastal risk for the next century, including sea level rise and changes in the coastline: application to charlestown ri, usa," *Natural Hazards*, vol. 88, no. 1, pp. 389–414, 2017.

Hamid, S., Kibria, B. G., Gulati, S., Powell, M., Annane, B., Cocke, S., Pinelli, J.-P., Gurley, K., and Chen, S.-C., "Predicting losses of residential structures in the state of florida by the public hurricane loss evaluation model," *Statistical methodology*, vol. 7, no. 5, pp. 552–573, 2010.

Hayward, S., "Development of a Realtime Wave and Storm Surge Forecasting Model for Rhode Island," University of Rhode Island," M. Eng. Thesis, July 2017.

Jonkman, S. N., Bočkarjova, M., Kok, M., and Bernardini, P., "Integrated hydrodynamic and economic modelling of flood damage in the netherlands," *Ecological economics*, vol. 66, no. 1, pp. 77–90, 2008.

Kerr, P., Martyr, R., Donahue, A., Hope, M., Westerink, J., Luettich, R., Kennedy, A., Dietrich, J., Dawson, C., and Westerink, H., "Us ioos coastal and ocean modeling testbed: Evaluation of tide, wave, and hurricane surge response sensitivities to mesh resolution and friction in the gulf of mexico," *Journal of Geophysical Research: Oceans*, vol. 118, no. 9, pp. 4633–4661, 2013.

Lee, K. H. and Rosowsky, D. V., "Fragility assessment for roof sheathing failure in high wind regions," *Engineering Structures*, vol. 27, no. 6, pp. 857–868, 2005.

Li, Y. and Ellingwood, B. R., "Hurricane damage to residential construction in the us: Importance of uncertainty modeling in risk assessment," *Engineering structures*, vol. 28, no. 7, pp. 1009–1018, 2006.

Li, Y., van de Lindt, J. W., Dao, T., Bjarnadottir, S., and Ahuja, A., "Loss analysis for combined wind and surge in hurricanes," *Natural hazards review*, vol. 13, no. 1, pp. 1–10, 2011.

Luettich, R., Westerink, J., and Scheffner, N., "ADCIRC: an Advanced Three-Dimensional Circulation Model for Shelves, Coasts, and Estuaries, Report 1: Theory and Methodology of ADCIRC-2DDI and ADCIRC03DL," U.S. Army Engineers Waterways Experiment Station, Tech. Rep. Dredging Research Program Technical Report DRP-92-6, 1992.

Mattocks, C. and Forbes, C., "A real-time, event-triggered storm surge forecasting system for the state of north carolina," *Ocean Modelling*, vol. 25, no. 3-4, pp. 95–119, 2008.

NHC. NOAA. "NHC data archive." 2018. [Online]. Available: https://www.nhc.noaa.gov/data/

NOAA. "Annual exceedance probability curves." Oct. 2013. [Online]. Available: https://tidesandcurrents.noaa.gov/est/curves.shtml?stnid=8452660

NOAA, "Sea Level Rise Viewer," 2018. [Online]. Available: https://coast.noaa.gov/digitalcoast/tools/slr

Oakley, B., "Generalized 1Quonochontaug Barriers, Rhode Island," Rhode Island: Shoreline Change Special Area Management Plan, Tech. Rep., 2016.

Parris, A., Bromirski, P., Burkett, V., Cayan, D., Culver, M., Hall, J., Horton, R., Knuuti, K., Moss, R., Obeyeskera, J., Sallenger, A., and Weis, J., "Global Sea Level Rise Scenarious for the United States National Climate Assessment," NOAA, Tech. Rep., 2012.

Pinelli, J.-P., Pita, G., Gurley, K., Torkian, B., Hamid, S., and Subramanian, C., "Damage characterization: Application to florida public hurricane loss model," *Natural Hazards Review*, vol. 12, no. 4, pp. 190–195, 2011.

Ris, R., Holthuijsen, L., and Booij, N., "A third-generation wave model for coastal regions: 2. verification," *Journal of Geophysical Research: Oceans*, vol. 104, no. C4, pp. 7667–7681, 1999.

Roelvink, D., Reniers, A., Van Dongeren, A., de Vries, J. v. T., McCall, R., and Lescinski, J., "Modelling storm impacts on beaches, dunes and barrier islands," *Coastal engineering*, vol. 56, no. 11-12, pp. 1133–1152, 2009.

Scawthorn, C., Flores, P., Blais, N., Seligson, H., Tate, E., Chang, S., Mifflin, E., Thomas, W., Murphy, J., Jones, C., *et al.*, "Hazus-mh flood loss estimation methodology. ii. damage and loss assessment," *Natural Hazards Review*, vol. 7, no. 2, pp. 72–81, 2006.

Schambach, L., Grilli, A. R., Grilli, S. T., Hashemi, M. R., and King, J. W., "Assessing the impact of extreme storms on barrier beaches along the atlantic coastline: Application to the southern rhode island coast," *Coastal Engineering*, vol. 133, pp. 26–42, 2018.

Small, C., Blanpied, T., Kauffman, A., O'Neil, C., Proulx, N., Rajacich, M., Simpson, H., White, J., Spaulding, M. L., Baxter, C. D., *et al.*, "Assessment of damage and adaptation strategies for structures and infrastructure from storm surge and sea level rise for a coastal community in rhode island, united states," *Journal of Marine Science and Engineering*, vol. 4, no. 4, p. 67, 2016.

Smith, J. M., Sherlock, A. R., and Resio, D. T., "Stwave: Steady-state spectral wave model user's manual for stwave, version 3.0," Engineer Research and Development Center Vicksburg, MS Coastal and Hydrualics Lab, Tech. Rep., 2001.

Spaulding, M., Isaji, L., Damon, C., and Fugate, G., "Application of STORMTOOLS's simplified flood inundation model, with and wihtout sea level rise, to RI coastal waters," *ASCE Solutions to Coastal Disasters Conference, Boston, MA*, Sept. 2015.

Spaulding, M., Grilli, A., Damon, C., Crean, T., Fugate, G., Oakley, B., and Stempel, P., "STORMTOOLS: Coastal environmental risk index (CERI)," *Journal of Marine Science and Engineering*, vol. 4, no. 3, p. 54, aug 2016.

Tomiczek, T., Kennedy, A., and Rogers, S., "Collapse limit state fragilities of wood-framed residences from storm surge and waves during hurricane ike," *Journal of Waterway, Port, Coastal, and Ocean Engineering*, vol. 140, no. 1, pp. 43–55, 2013.

Torres, M., Hashemi, M. R., Hayward, S., Spaulding, M., Ginis, I., and Grilli, S., "The Role of Hurricane Wind Models in the Accurate Simulation of Storm Surge and Waves," *ASCE Journal of Waterway, Port, Coastal and Ocean Engineering Online Collection*, vol. in review, 2017.

USACE. "North Atlantic Coast Comprehensive Study. Resilient Adaptation to Increasing Risk." Jan. 2015. [Online]. Available: http://www.nad.usace.army.mil/Portals/40/docs/NACCS/10A_PhysicalDepthDmgFxSummary_26Jan2015.pdf

Vickery, P. J., Skerlj, P. F., Lin, J., Twisdale Jr, L. A., Young, M. A., and Lavelle, F. M., "Hazus-mh hurricane model methodology. ii: Damage and loss estimation," *Natural Hazards Review*, vol. 7, no. 2, pp. 94–103, 2006.